UNIVERSITÀ
DEGLI STUDI
DI PADOVA

Università degli Studi di Padova

Dipartimento di Ingegneria Industriale DII

Corso di Laurea Magistrale in Ingegneria Meccanica

SURFACE QUALITY ANALYSIS OF POST-CONSUMER RECYCLED POLYPROPYLENE

Relatore:
Prof. Giovanni LUCCHETTA

Laureando: Mattia AMBRA
Matricola: 1241332

ANNO ACCADEMICO 2022/2023

A mia madre

come ieri, come domani

Ringraziamenti

Voglio ringraziare tutte le persone che mi sono state vicine in questi difficili anni che sono coincisi con il mio percorso di laurea magistrale.

Innanzi tutto, un grazie va alle mie sorelle Elisa e Greta, con le quali siamo riusciti ad andare avanti nonostante la terribile esperienza che abbiamo dovuto vivere.
Grazie anche a mia cugina Arianna e le zie Emilia, Marilisa e Laura, che ci sono sempre state.

Grazie agli amici che conosco ormai da una vita Luca, Andrea e Fabio per essere stati una costante nella mia vita che mi ha sempre rasserenato.

Grazie agli amici che ho incontrato in questo alquanto lungo percorso universitario. Ad Andrea e Mauro, con i quali è bello condividere molte delle mie passioni. A Giacomo, Enrico e Matteo, con cui ho passato veramente tanto tempo tra una lezione e l'altra. A Giulio, che per molti versi mi ha fatto riscoprire il giusto modo di affrontare il percorso universitario. A Manuela e Fabrizio, per aver condiviso molte esperienze in laboratorio. E ad Alessandro, nonostante le nostre vite ci abbiano portati a vivere molto distanti.

Grazie, infine, agli amici che in un modo o nell'altro sono entrati a far parte della mia vita come una famiglia. Alle ragazze di casa questura Francesca, Anna Rita e Lucia ed a tutti i membri della gaycrew con i quali ci trovavamo praticamente per tutte le festività. Grazie ai miei attuali e passati coinquilini Matteo, Caterina, Martina, Margherita, Marco, Stella, Anna e Marialuisa per aver reso bello il vivere assieme. E grazie ad Alberto e Valentina, amici inaspettati, ma comunque molto cari.

Senza di voi sarebbe stato tutto molto più difficile.

Abstract

The behavior of post-consumer recycled Polypropylene for aesthetic purposes was investigated. In order to do that, the most influent processing parameters in terms of surface defectiveness were identified and then varied following a Multifactorial Design of Experiment.

After the samples were obtained according to the experimental plan, a series of photos was collected of their surfaces. The photos were then processed using the OpenCV python library.
The first step of the image processing was to establish an object detection algorithm to locate the area of the images in which only the sample's surface was present.
Then, once the sample's surface was identified in all the photos, an edge detection algorithm was used to highlight the borders of the defects present on the surface. After that a defectiveness index was defined for each sample from the image representing the edges.

With the indices measured from the photos and through the means of data analysis, the influence of each parameter and their mutual interactions were studied on the surface defectiveness.
Firstly, an analysis of variance was performed to identify which parameter variations were statistically significant.
Then, the Main Effects and the Mutual Interactions plots were individually analyzed. This allowed to assign to each parameter and each interaction its corresponding influence in terms of defectiveness index.
A Linear Regression Model to forecast the defectiveness of new samples obtained in new processing conditions was finally built using the data collected in the experiments.

In the last pages, a possible correlation between the conditions that lead to more surface defectiveness and the mold wall's contamination was investigated. To do so,

data about machine operating conditions and contamination was collected in collaboration with FHP establishment in Monselice.

SUMMARY

Introduction

Problem exposition

The transition to a sustainable and circular plastics economy demands focus, collaboration and sizeable, long-term investments in systems and technology that can deliver the transition to a zero-waste future. In the recent past, a big obstacle to this transition was represented by the visual appearance of objects manufactured by using post-consumer recycled plastics.

Nowadays, visual appearance of manufactured products is crucial in determining the final costumer choice: phone covers, car interiors and PC or TV encasings are just some of many examples.

The presence of surface defects lowers the final product perceived quality, leading to product rejection even though the defect has no impact on functionality. (Marielle E. H. Creusen, Jan P. L. Schoormans, 2005)

Moreover, depending on the cause that is responsible for the defect formation, some issues can emerge in the manufacturing process regarding contamination or degradation of the machinery used. These problems need to be addressed, because they lead to more frequent idle times to allow cleansing and replacement.

Lastly, the process that originates the defects, while not changing the macroscopic behavior of the final product, may change its surface roughness; this needs to be accounted for in some use cases.

Injection Molding

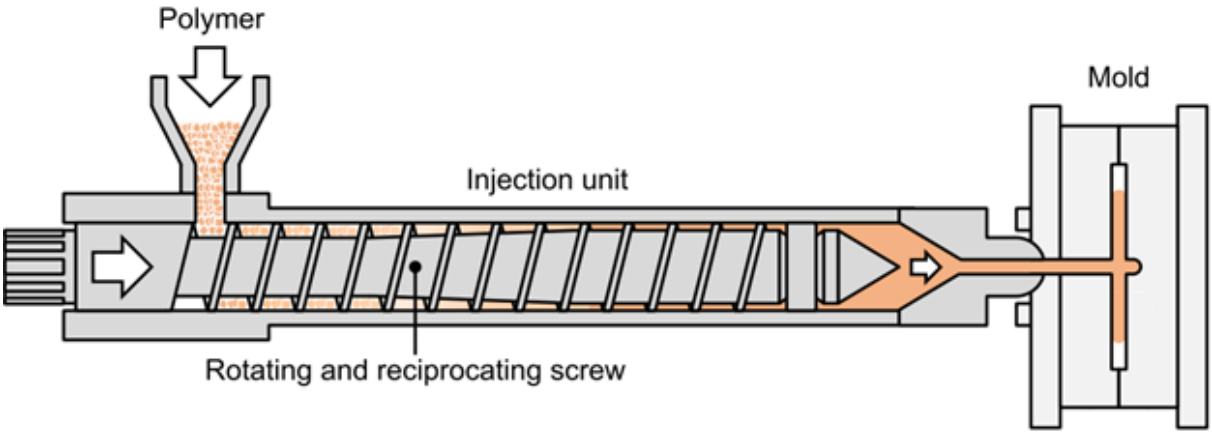

Fig. 1: Injection Molding Machine Model

Injection Molding is the most popular technique used in mass-production of polymeric parts with complicated geometry, consistent quality, and attractive appearance.
It consists in melting some polymeric pellets by viscous heating:

- The pellets are introduced inside a barrel
- The screw inside the barrel moves back while rotating, making the polymer advance towards the screw head. This movement induces friction on the pellets, that are deformed and melt as they proceed inside the barrel
- Once enough material is stored in the barrel head, the screw stops rotating and pushes the molten polymer through a nozzle inside a Mold
- After the Mold is completely filled, the screw keeps pushing, maintaining a pre-set holding pressure to introduce new material that compensates for thermal shrinkage
- After enough time has passed to guarantee the structural integrity of the solidified product, the Mold is opened, and the final product is extracted

Polypropylene Recycling

Recycling Process

There are mainly two different ways to recycle a thermoplastic material:

1. Mechanical Recycling - is the most common approach used for recycling plastics; it refers to the processing of plastics waste into secondary raw material without significantly changing the material's chemical structure. In principle, all types of thermoplastics can be mechanically recycled with little impact on quality, but this only happens if the material collected from post-consumption is perfectly sorted and does not contain contaminants
2. Chemical Recycling - is a growing approach for recycling and offers greater opportunity for scalability; it covers a set of technologies (pyrolysis, gasification, hydro-cracking, depolymerization) that change the chemical structure of plastic waste. Long hydrocarbon chains constituting plastics are broken into shorter hydrocarbon fractions or monomers using chemical, thermal, or catalytic (chemical/thermal) processes. These shorter molecules are ready to be used as feedstock for new chemical reactions to produce new recycled plastics and other chemicals. (PlasticsEurope)

There are major differences between chemical and mechanical recycling. In mechanical recycling, plastic degrades over time due ultraviolet light and other environmental conditions. Additionally, as plastic is ground and melted during mechanical recycling, the polymer chains are partially broken down. Both of these factors reduce its tensile strength and viscosity, making it more difficult to process. Moreover, contaminants are introduced in the recycled material due to the recycling process characteristics, altering the macroscopic thermo-mechanical properties. This lower grade plastic can only be recycled a limited number of times before its altered physical properties make it unusable for plastic product containers.

Chemical recycling is an infinite loop. Plastic recycled this way can be processed over and over again without any reduction in physical properties. This is because the waste is not just being cleaned and reheated, but it is being used as feedstock into a chemical

process which transforms it back to ethylene molecules and then ultimately into the exact same specified plastic used for the original package. (DrugPlastics, 2022)
Even though Chemical recycling seems to be the better option, it is still less popular. This is mainly due to the higher costs, as separating plastics into different polymers is easier and way cheaper than degrading it into monomers. With modern technologies, this process requires lots of energy and costly machinery. Moreover, the fact that chemical recycling is a relative new technology in respect to mechanical recycling means that not enough advancements in research were made to make it competitive in costs.
Ideally, both these two recycling techniques shall be implemented in order to achieve an optimal circular economy: mechanical recycling as it is a nice compromise between material degradation and energy/cost effectiveness, and chemical recycling as a mean to regenerate virgin polymers out of materials that would not be good to mechanically recycle anymore.

Mechanical Recycling Stages

Mechanical Recycling can be divided into 6 different stages:

Collection: it is a vital phase for the purpose of circular economy. By separating waste correctly at the point of collection, the recycling process is more efficient and will increase the quality and quantities of recycled products. Improved waste collection positively impacts the waste streams and their suitability for downstream pre-treatment, sorting and recovery operations.

First Sorting: once plastic arrives to the recycling plant, it is sorted into different polymers. While some sorting may have taken place at the collection stage, further separation by color or thickness may be necessary. A wide range of technologies are currently used for waste pre-treatment and sorting. These range from manual dismantling and picking to automated processes. Modern sorting plants are complex facilities that apply several technologies adapted to specific waste streams to achieve

optimum cost-effective output, producing sorted waste with a purity higher than 95% for some plastics.

Shredding: after a first sorting, plastic products are shredded into small pieces to facilitate the successive washing, final sorting and melting stages

Washing: Washing removes dust and dirt to ensure plastics are clean before they go onto the next stage. This can include removing traces of food, drink or labels.

Second sorting and control: a second sorting, executed after shredding and washing, allows for a better recognition of any extraneous material that was left after the first sorting.

Extrusion: plastic flakes are melted and converted into homogeneous pellets, ready to use in the manufacture of new products

(PlasticsEurope)

Mechanically Recycled Material Properties and Issues

Due to high demands for sustainability in polymer engineering, the usage of recycled polymer materials is increasing. However, recycled polymer materials have been limited in the application for aesthetic parts due to the inferior surface quality resulting from their implementation. (Jinsu Gim, Lih-Sheng Turng, 2022)
This is caused by the lower material homogeneity that is intrinsic to the production of mechanically recycled polymer materials: pellets resulting from this process will contain, together with the base polymer, both other kinds of polymers and additives. The presence of extraneous material causes the recycled polymer to behave differently from the virgin one. Moreover, some additives can thermally degrade, determining the presence of gas in the melt, which causes surface defects.
As there is no easy way to determine the final thermo-mechanical properties of the pellets obtained from mechanical recycling, the virgin material properties must be

taken as reference in the conceptualization phases of any activity involving recycled plastics.
In the following dissertation, the processing parameters for injection molding of post-consumer recycled Polypropylene are selected in the same range as for virgin-Polypropylene.

Literature about photo acquisition and image processing

At this moment in time, very few research is published regarding the application of Image Processing techniques on Surface Analysis in manufacturing industry. The main effort has been put on measuring the surface roughness and using it as a proxy for the presence of defects. This method is based on the assumption that the observed defects are caused by gases present in the molten fluid, that are pushed to the mold walls and dragged along the flux lines; this determines different cooling conditions where the gas bubbles are present, forming a valley on the surface for each bubble. (Jinsu Gim, Lih-Sheng Turng, 2022)
In February 2023 *Jinsu Gim, Huaguang Yang and Lih-Sheng Turng* published an article in which they developed a model to detect surface defects for Transfer Learning between different machinery. In the article, to detect the presence of defects on the surface of a sample the following procedure was used:

1. The photo was converted to grayscale (each pixel was assigned a value from 0 to 255)
2. The brightness of the image was normalized by standard white and standard black using as reference a perfect diffusing surface and a perfect absorbing surface included in the photo
3. A median filter was applied to filter noise in the image
4. A copy of the image was created, which was then heavily blurred to extract the base color of the sample
5. The surface defects were revealed subtracting the blurred copy to the filtered image
6. The severity of the defects was represented by the standard deviation of the values assigned to the pixels of the image resulting from the subtraction

7. A threshold value was defined for the standard deviation: values higher than the threshold referred to defective sample, values lower were considered as non-defective

(Jinsu Gim, Huaguang Yang, Lih-Sheng Turng, 2023)

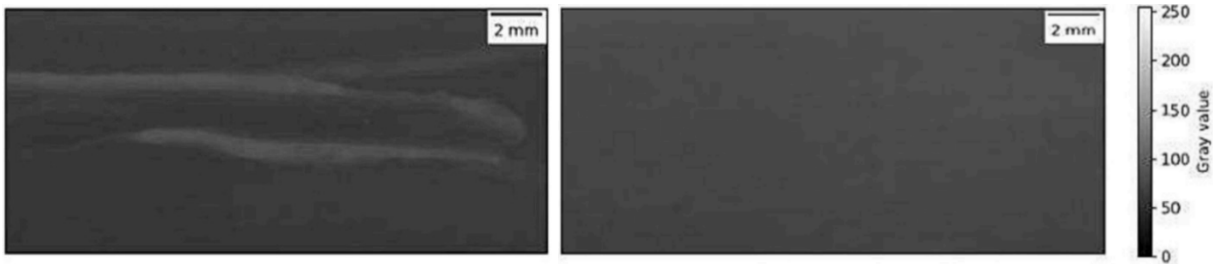

Fig. 3: on the left greyscale of the image after median filtering, on the right the same area after gaussian blurring

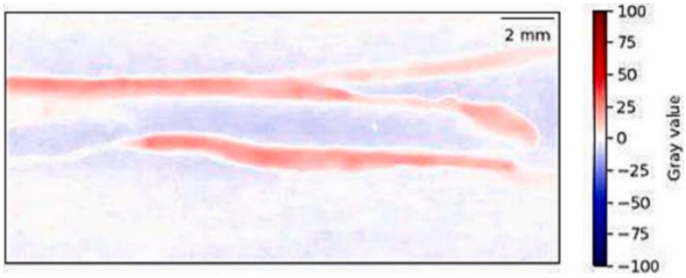

Fig. 2: image obtained after subtracting the blurred background from the original grayscale image

Linear Regression Models and Statistical Data Analysis

A designed experiment is a test (or a series of test) in which input parameters are purposely changed in order to observe and identify corresponding changes in the output response.

In this dissertation, the experiments were conducted following a *Multifactorial Design of Experiments*. It consists in:

- Choosing the input parameters, of which we want to study the effects: X_1, X_2, …, X_n
- Choosing the levels over which the input parameters are varied
- Choosing a significative output variable that is going to be monitored to evaluate the effects of the input parameters: Y
- Perform a series of experiments, with all the possible combinations of the different levels of the monitored parameters

This design is particularly useful for screening the variables in a process to determine those that are most important.

Experimental Phase

The objective of this research has been to tackle the main critical point that inhibits the large-scale adoption of post-consumer Recycled Polypropylene for aesthetic purposes, which is the frequent presence of defects on the surface of objects obtained using this material.

To do so, the first step was to identify all the parameters that could be influencing the final object aesthetic. A *Multifactorial Design of Experiment* was then used to create an experimental plan with all the possible combination of the chosen parameters. With the processing parameters settings provided by this plan a set of 3 samples was injection molded for each combination.

After this, it was identified a method to evaluate the severity of the defects present on each sample's surface. This was done by acquiring a photo of each sample, processing it via image processing algorithms and defining a defectiveness index.
The index so defined was used to create a regression linear model, to find out how the chosen processing parameters influence the surface defectiveness. To determine which parameters were to be included into the regression model, the data obtained from the experiments were analyzed with the statistical tools provided by the Minitab software and Python.

Finally, a possible relation between the surface defectiveness and the layer of dirt that forms on the mold walls while processing this material was investigated.

Injection Molding Machine description

The samples were obtained using a *Battenfeld HM 110 / 525H / 210 S* Injection Molding machine.

Fig. 4: Photo of a Battenfeld Injection Molding Machine

The clamping unit of this machine is capable of a clamping force up to 1100 kN. The cylinder diameter is 25 mm. For this diameter, the maximum theoretical shot volume is 73,6 cm^3 and the maximum injection pressure is 2940 bar.

For the experiments it was used a mold with very simple geometry.
A *Heat Chamber* separates the sprue from the mold.
Even though there are two possible injection points in the cavity, one was closed. This eliminates the chance of having weld lines formation in the middle of the piece, at the cost of higher pressure loss inside the cavity and doubling the injection time.

Sample Description

The sample chosen to conduct the experiments has a very simple geometry: it is almost flat and is composed of a rectangular shape (14,5 cm x 5 cm) with two triangles at its extremes.

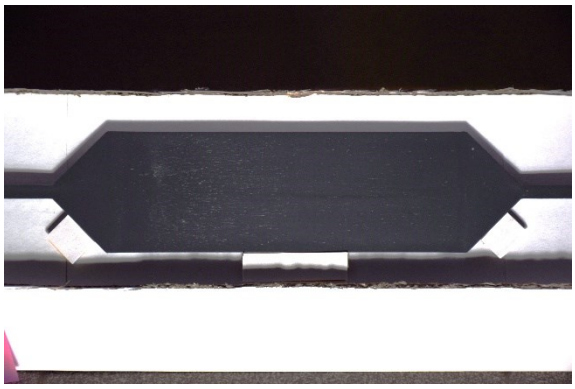
Fig. 5: Photo of the sample

The triangular portion of the sample only serves to distribute the material along the

sample's section. Then only the rectangular portion of the sample will be object of this study.

Multifactorial Parameters Choice

To build a significant regression model that is able to predict the presence of defects on the surfaces of samples obtained from recycled-Polypropylene, the most influent processing parameters must be chosen as the variables of the model.
In the following paragraphs the monitored parameters are presented, explaining the reasons why they were chosen and the way the ranges were determined for each parameter.

Injection Rate

The Injection Rate is the amount of volume of melt material injected in the Mold in a unit of time. It is measured in cubic centimeters per second *[ccm/s].*
Injection Rate is crucial in determining whether Surface Defects will be present on the sample. Higher Injection Rates make so that a lot of frictional heating is generated when the melt is injected into the cavity through the nozzle; this makes the melt hotter, and combined with the fact that the cavity is filled up quicker, ends up in more homogeneous cooling conditions of the material throughout the mold.
When lower injection rates are used, the filling time gets longer and it has been observed that the liquid viscosity gets higher very quickly. The combination of these two factors results in the fact that material
initially injected into the cavity cools down rapidly, meaning that higher pressure is needed for the subsequent phases of the injection and possibly the cavity will be filled unevenly. (Jian Wang, Qianchao Mao, Nannan Jiang, Jinnan Chen, 2021)
More often than not, the low-speed injection of molten material leads to a long filling time and produces products highly prone to defects like uneven density, weld lines, as well as large residual stress. (KBdelta, s.d.)

Given these considerations, two levels were chosen for Injection Rate, to evaluate the difference between low flow rates and higher ones.

	LOW	HIGH
Q_{in} [ccm/s]	10	30

Table 1: Chosen levels for Injection Flow Rate

Backpressure

Backpressure is the pressure to which is the molten polymer is kept during the metering phase. It is controlled setting how restrictive the return valve will be as the hydraulic fluid returns to the hydraulic fluid tank during screw recovery.

It is generated by the plastic itself: as the screw rotates, the pressure of the plastic in front of the screw builds up; once that plastic generates enough pressure to exceed the pressure required to force hydraulic fluid through the proportional return valve, then the screw begins to retract its position.

Backpressure is calculated by taking the hydraulic pressure inside the valve and multiplying it by the *intensification ratio*, which is the ratio between the diameter of the hydraulic piston pushing the screw and the screw diameter itself. *Even though this does not take into account the non-Newtonian behaviour of molten polymers, it is still a good enough way to keep track of backpressure regardless of the processed polymer or its Temperature.*

From the polymer point of view, a higher Backpressure means higher levels of deformation stresses, resulting in more heat added to the material and possibly lower density of the fluid in the shot volume. A higher backpressure guarantees better melt uniformity, too. (Robert Gattshall, 2022)

Backpressure is usually set between 35 to 70 bar, but higher levels can be used if more heat need to be introduced in the fluid or the melt is not adequately uniform. In case the processing material contains fibres, backpressure should not exceed 20% of the injection unit capacity to prevent glass fibre breakage. (AshaiKASEIplastics, 2018)

For backpressure, two levels were chosen to represent the two extremes of the suggested range. Some experiments were run with much higher values (140 bar), which resulted in way longer

	LOW	HIGH
p_b [bar]	35	70

Table 2: Chosen levels for Backpressure

Melt Temperature

For virgin-Polypropylene pellets, the Melting Point is reached at 166 °C. *(Jian Wang, Qianchao Mao, Nannan Jiang, Jinnan Chen, 2021)*. The target Melt Temperature for Injection Molding is between 190 and 250 °C.

To control the Melt Temperature, an ascending profile is chosen for the Temperatures of the various cylinder zones. The polymer enters the cylinder in the feeding zone, which is kept at 60 °C, and is gradually heated as it goes through the various zones. The cylinder zones on the screw head are set to the Target Temperature.

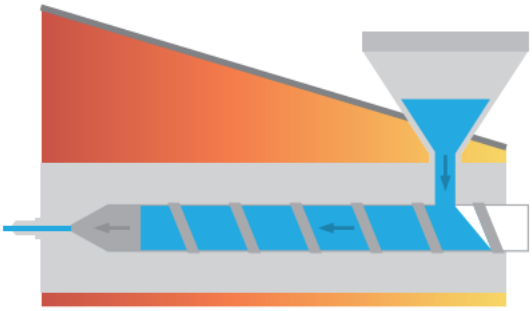

Fig. 6: Ascending Cylinder Temperature diagram

Too low Temperatures can promote flow marks, weld lines, poor surfaces, lamination, and short shots. This is caused by parts of the injected fluid that solidify too soon.

Too high of a Temperature can cause problems with flashing and burning and with shrink phenomena such as sinking, warpage, shrinkage, and void formation. (AshaiKASEIplastics, 2018)

For the post consumer Recycled Polypropylene, one more problem the arises when setting Melt Temperature is that additives are present in the processed pellets. Those additive, especially organic ones, can degrade at high Temperature, resulting in the presence of gases inside the fluid.

As the additive degradation is a Thermically activated process, it increases exponentially with Temperature and Residence Time.

Temperature levels are chosen at the extremes and in the middle of the suggested range, in order to return a decent representation of how Temperature affects Surface defects in all its domain.

	LOW	MEDIUM	HIGH
T_m [°C]	190	220	250

Table 3: Chosen levels for Melt Temperature

Drying Time

As polypropylene is not hygroscopic, it is unaffected by moisture content. Moisture contents up to 0.2% do not affect the physical properties of polypropylene in moulded parts, so drying is not typically required.

However, if the resin contains mineral or bio fillers, the likelihood of moisture absorption increases. This is the case of post-consumer Recycled-PP, as the many additives present in it will absorb a relevant amount of humidity from the air. (AshaiKASEIplastics, 2018)

To remove the humidity absorbed, it is suggested to keep the pellets at 90 °C in a drier for 90 minutes.

Experiments were performed both with and without previous pellets' drying. This is done to single out the influence of the additives' degradation on Surface Defects and to see how humidity compounds with it.

	LOW	HIGH
t_d [min]	0	90

Table 4: Chosen levels for Drying Time

Cycle Time

As material degradation increases with time spent at a certain Temperature, Cycle time was used as a proxy to evaluate how much time was spent from the molten polymer inside the high Temperature zones of the cylinder.

Cycle time was artificially changed in two ways:

- To reduce it to 48 s, metering was delayed by 12 seconds. This is the least amount of time that the machine used could invest to produce the piece, as metering needs to happen while the solidified piece is cooling inside the mold. As cooling is set to take 27 seconds and metering happens in just less than 15 seconds, metering can be delayed of 12 seconds maximum
- To increase it to 120 s, 60 seconds were spent idle between an injection and the other. Doubling Cycle time in this way simulates having double the amount of molten polymer on the screw head, half of which does not get injected into the mold and is kept an entire cycle time more at the highest Temperature

	LOW	MEDIUM	HIGH
t_c [s]	48	60	120

Table 5: Chosen levels for Cycle Time

Factorial Design recap

The table underneath contains all the chosen levels for the selected parameters. During the data acquisition campaign, a set of 3 samples was created with every possible combination of these parameters.

While changing Backpressure and Injection rate between two cycles rose no problems, changing the other parameters (especially Melt Temperature and Drying Time) meant that produced pieces needed to be discarded until regime conditions were achieved.

Injection rate Q_i [ccm/s]	Backpressure p_b [bar]	Melt Temperature T_m [°C]	Drying time t_d [min]	Cycle time t_c [s]
10	35	190	0	48
		220		60
30	70		90	
		250		120

Table 6: Summary table of all the chosen levels

Other constant parameters

Injection pressure

Injection pressure controls the rate at which the material enters the mould. Based on the required fill pressure, an additional 10% should be available on high setting. This should be applied for 99% of ram travel during the filling phase to maintain control of fill velocity. Too much pressure can cause parts to flash, burn, and stick in the mould. This means having high enough Injection pressure is crucial to effectively control Flow Rate levels, which is a parameter monitored in our DOE.

An Injection pressure of 1100 bar was chosen.

Packing pressure

Packing pressure affects the final part aesthetics. When packing pressure is applied evenly, it controls sink marks and shrinkage.

A packing pressure of 450 bar was chosen for all the experiments.

Packing time

Packing pressure should be applied until the gate freezes off or when consistent part weight is achieved.

As the produced sample is very thin and the differential between maximum Melt Temperature and Melting Temperature is *250 - 166 = 84 °C*, it was observed that applying Packing pressure for 12 seconds was enough.

Mold Temperature

Mould temperatures usually are in the range 20 – 60 °C. Temperatures should be high enough to produce good part surfaces and to avoid flow marks, weld lines, lamination, brittle parts, voids, short shots, and core sticking. Temperatures should not be so high however, that shrinkage, warpage, sinking, and cavity sticking become problems. Cooling the mould should be uniform unless differential cooling is needed to reduce part warpage.

For applications where aesthetics are critical, a surface temperature of 80-95˚C is suggested, even though this means longer cycle times.

A Temperature of 50 °C was chosen, as the experiments wants to emulate typical production conditions, with contained cycle times. This value is in the high part of the 20 – 60 °C range, as we wanted to assure that no surface defects could be attributed to the mould Temperature.

Cooling time

Cooling time allows to cool the part before removing it from the mould, preferably at about 60 °C. Shortening the cooling time increases warpage. Sinking and shrinkage also increase if the cure time is shortened.

During the experiments, cooling time was set to 27 seconds. This, in combination with the mould Temperature, made so that the final piece had sufficient structural resistance when extracted and no shrinkage was visible.

Metering volume

At the end of each cycle, the screw was retracted to have 44 cubic centimeters of molten plastic on its head. This value was chosen as it left a small enough cushion of melt material after injection and was high enough not to have short shots occur.

Image Acquisition and Image Processing

Photo Acquisition

To evaluate the severity of the surface defects present on the surface of the samples created following the Experimental Design, it was chosen to make use of Computer vision algorithms that developed in the last decades.

Camera and camera settings

The device used to acquire photos of all the samples was a *Nikon D5300* camera, which is a 24 megapixel digital single-lens reflex camera.

Fig. 7: photo of a Nikon D5300 camera

This camera's 24 megapixel allow to acquire images with a resolution of 6000x4000 pixels. The ISO sensitivity can be changed in a range from 100 up to 25600 and the shutter speed can vary from 1/4000 s to 30 s.

It has a 640x480 pixels LCD screen to easily navigate between the camera settings and replicate what is seen looking into the camera scope.

The camera can also be used as a tethering hotspot, allowing to change camera focus and take photos through a wireless device. This is particularly useful for our experiment's objective, as not touching the camera in between photos ensures the photos are as similar as it gets.

Photoset

The photos were taken in a dark room, that was completely obscured from outer light sources by masking all the windows and closing all the doors.

As the samples needed to be held all in a similar position, a support was built to keep them in place. The support needs to be uniformly colored of a color that is clearly different to the color of the samples. A heavy weight was put on its top to keep it from moving while the samples were replaced.

To guarantee a good enough repeatability of the observations, the photoset had to be arranged in a way to satisfy the following requisites:

Fig. 8: photoset

- The camera lens have to be parallel to the surface, to represent all the surface in the most homogeneous way possible
- The longest side of the sample has to be aligned with the longest side of the photo; this allows to get closer to the sample while still managing to entirely fit it into the photo, enhancing the resolution of the surface
- The light source must come from a 45° angle; in this way the reflected light is not directed straight to the camera lens, which would cause to have light spots on the photo

One more thing to be wary about is to position the light source far enough from the sample. This is done so that the light can reach every point of the sample with a similar intensity. If the light distribution over the sample surface is not satisfactory, a white

panel can be placed between the light source and the support; this trick gives better light diffusion, at the cost of reducing the overall intensity.
After having prepared all the setup, every photo was shot making use of the wireless tethering of the camera. This function creates a wireless network hosted by the camera, to which any device like a laptop or a mobile phone can join. Through this wireless connection the focal point of the camera can be changed and the trigger to take the photo can be given remotely, without the need to touch the camera.
By limiting the number of times the camera needs to be directly operated on, it was ensured that all the photos had very slight differences in where the samples were located, simplifying greatly the successive object location phase.

Image Processing

After the photos of all the samples were acquired, they were transferred from the SD card inside the camera to a computer to be analyzed.
The first step in this analysis has been to identify a procedure that automatically locates the sample inside the photo, so that it can isolate it and crop it out.
Then, it was defined a procedure to elaborate the cropped samples in a way to obtain a defectiveness index, which gives an esteem of how severe the presence of defects on each sample is.
All the Image Processing steps were performed writing a Python code that mainly used the *OpenCV* and *Numpy* libraries.

Image Mask and Object Detection

First of all, as precautions were used to ensure that the samples were located more or less in the same part of the photos, a smaller area of the images was cropped in such a way that all the flat surfaces of the samples in all the photos were surely inside it. This allowed to reduce the images from 6000x4000 pixels to 4300x1750 pixels, cutting the amount of data that needed to be processed to less than a third, thus improving the processing speed.

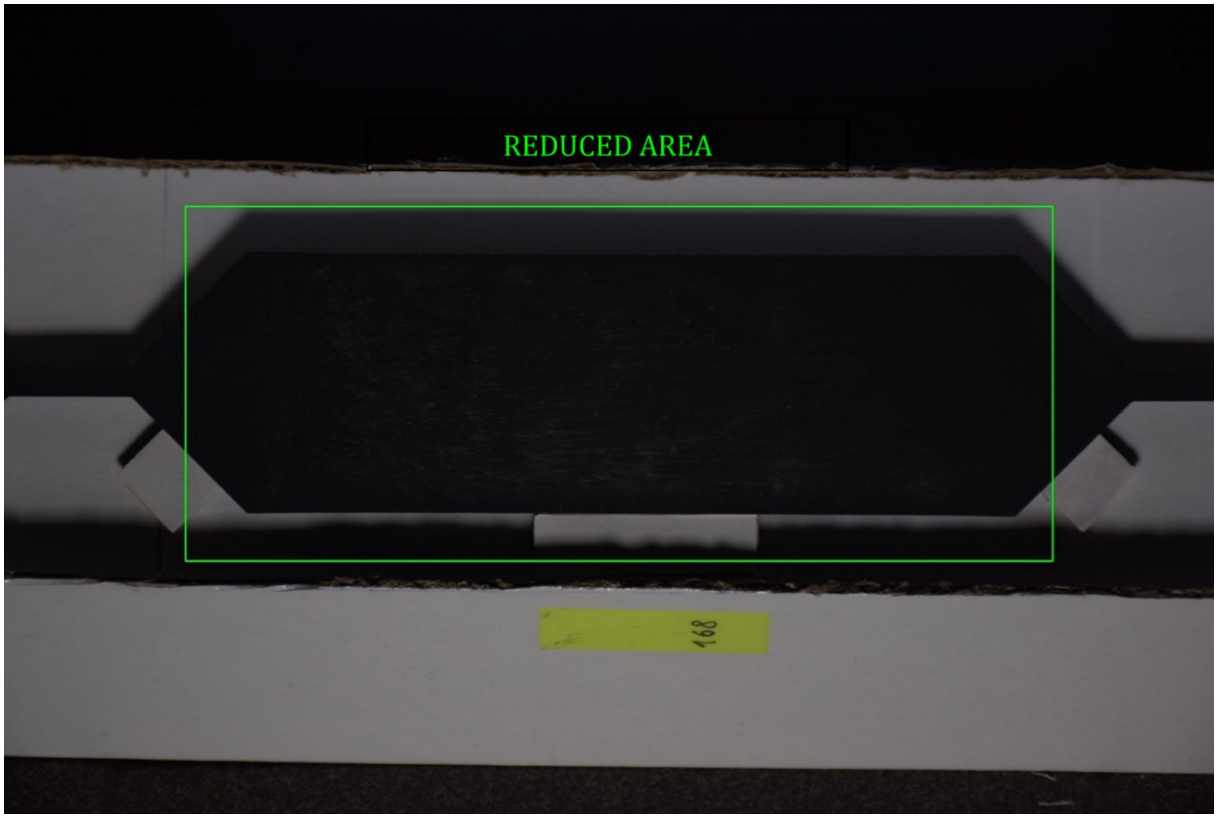

Fig. 9: Original acquired photo with the reduced area highlilghted by a green rectangle

To obtain a mask that replicates the shape of the sample, the following procedure was used:

1. it was applied the *inRange* method of the OpenCV library on the reduced area
2. five iterations of the *Closing* morphological operator were performed
3. the *floodFill* method was used to change the color of the pixels belonging to the sample
4. the *where* method of the Numpy library was used to filter the pixels that were identified from the *inRange* method not belonging to the sample
5. if any point inside the resulting shape is not considered as belonging to the mask, its color is changed to become part of the mask
6. columns with a fraction of white pixels that is less than 95% of the maximum fraction were completely obscured

The *inRange* OpenCV method is a function that receives in input a *NxN* three levels matrix and returns a single level *NxN* binary matrix. Each pixel of the original-colored

image is represented in the input matrix by a 3D vector, which is the combination of the fundamental colors (Reg, Green and Blue from 0 to 255) present in that pixel.
This function checks if each pixel is inside or outside of a provided range, returning 255 if True and 0 if False. The values returned by this algorithm are then arranged to create a Black-White image that masks the pixels inside the provided range.

The *Closing* morphological operator is composed by a *Dilation* followed by an *Erosion*.
The *Dilation* expands objects inside the image: a copy of the input image is created, where each pixel is set to 255 if at least one its bordering neighbors (plus itself) was at 255 in the original image.
The *Erosion* reduces the dimension of the objects and removes the smaller details: it works in the same way as *Dilation*, but the rule is changed so that pixels are set to 0 if at least one its bordering neighbors (plus itself) was at 0 in the original image.
Morphological closing is useful for filling small holes in an image while preserving the shape and size of large holes and objects in the image. (MathWorks, s.d.)
In this particular case, it serves for two important functions:

- it straightens the borders of the sample, filling the holes left from the brightest spots that were located on the sample's contour
- it connects together all the pixels set at 255 belonging to the sample, preparing for the successive *floodFill* method

The *floodFill* method behaves in the following way: starting from a point chosen as input, it changes the color value from the original to another one; then, for all the bordering pixels, it checks if any of them has the same color value as the original starting point and, if so, changes their color value too.
To better understand the way this method works, the pixels of the image matrix can be imagined as a grid that subdivide the areas of a map: the ones with different color values from the originally selected one can be imagined at the ground level, while the ones that have the same color value are engraved to a lower level. When a bucket of water is spilled from the original point, the water floods all the areas that are directly connected to it, changing their level to another one; the ones that do not have a direct connection are left to their original value.

This method is used to single out only the pixels belonging to the sample's surface, as the *inRange* method may identify pixels even outside of this area. Their color value is changed to 125, differentiating them from all the other pixels in the mask, whose values remain set either to 0 or 255.

After having singled out only the pixels of the right color that belong to the sample, the *where* Numpy method is used to go back to a binary identification of the pixels, mapping the ones whose value is 125 to 255 and all the others to 0.

A control loop is then defined to check for each row of the mask matrix if there are any white pixels (set to 255) in it. If so, the pixels between the two most distant white pixels are set to 255, filling the holes that are left in the shape.
This loop is defined to check over each row and not each column because, given the orientation of the images, there are way less rows than columns, thus improving the computation speed for the loop.

Finally, as only the rectangular surface of the sample is object of this study, it was found the maximum amount of white pixels inside a column among every column. Then, the columns where the number of white pixels was less then 95% the maximum amount were completely turned to black.

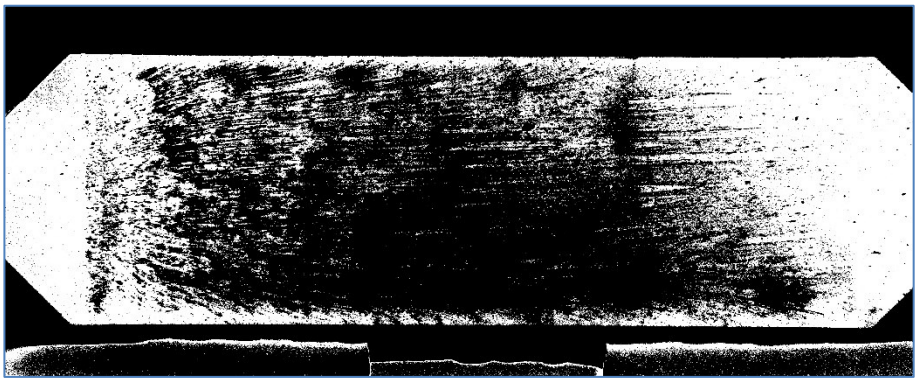

1) inRange function to identify pixels of the sample's color

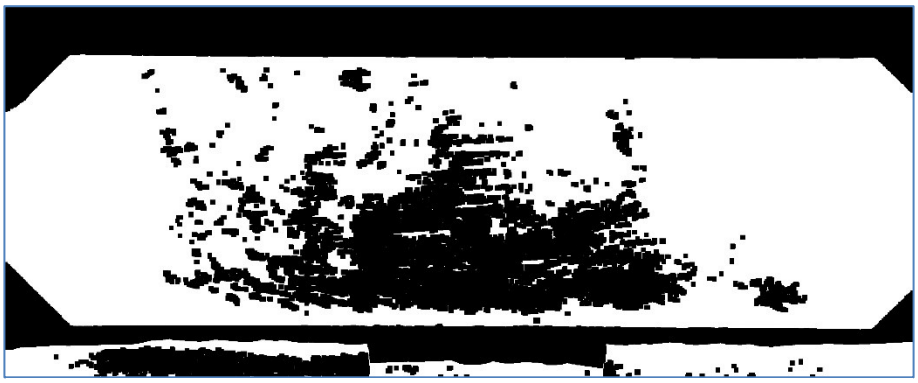

2) Closing morphological operator to connect the pixels inside the shape

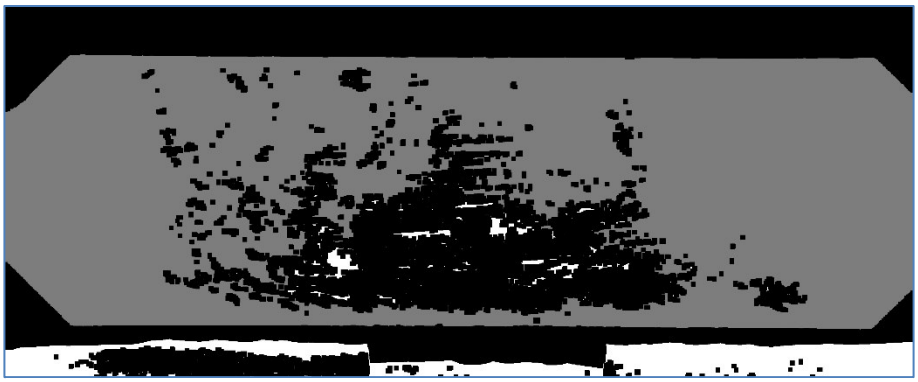

3) The connected pixels of the sample are singled out by changing their color

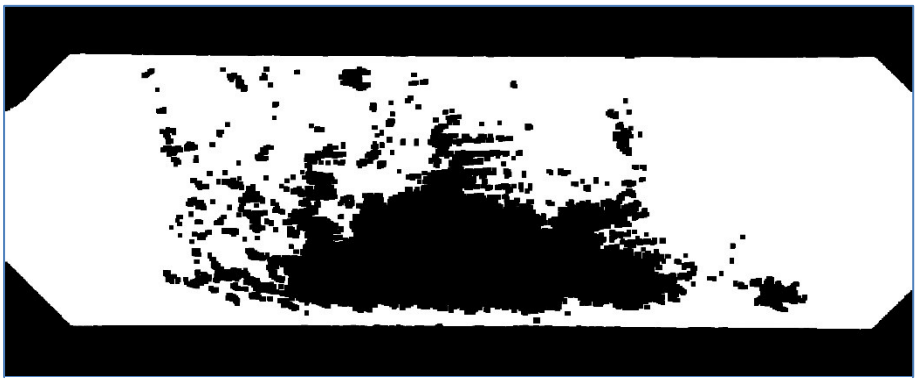

4) The mask is turned back to Black and White, where only the connected pixels belonging to the sample are white

5) The black spots inside the shape are all turned to white

6) Only the rectangular face of the sample is left unmasked

Edge Detection to identify Defects

Once a mask of the sample has been obtained, it can be applied to the original image, after it has been converted from RGB to Grayscale. This makes so that the successive operations can be performed considering only the area of the photos belonging to the sample.

To identify defects on the surface, it was chosen to use the *Canny* edge detection algorithm present in the OpenCV library. This is a multi-stage process, which is able to return a Black-White image matrix for an input Grayscale image matrix, where the pixels identified as edges are set to 255 and all the others to 0.

Step 1: **Noise Reduction**

To reduce noise in the image, a 5x5 Gaussian filter is applied to the image.

Step 2: **Finding intensity Gradient of the Image**

To perform this step, a Sobel operator is applied to the image along both the x-axis and the y-axis. The image gradient is then found applying Pitagora's Theorem and its direction is rounded to be horizontal, vertical or along the two diagonal directions.

$$G_x = \begin{bmatrix} -1 & 0 & +1 \\ -2 & 0 & +2 \\ -1 & 0 & +1 \end{bmatrix} \cdot I \qquad G_y = \begin{bmatrix} -1 & -2 & -1 \\ 0 & 0 & 0 \\ +1 & +2 & +1 \end{bmatrix} \cdot I$$

$$Edge\ Gradient\ (G) = \sqrt{G_x^2 + G_y^2} \qquad Angle\ (\theta) = arctg\left(\frac{G_y^2}{G_x^2}\right)$$

Step 3: **Non-maximum Suppression**

After getting gradient magnitude and direction, for each pixel it is checked if it is a local maximum in its neighborhood in the direction of gradient. Take the following image as an example:

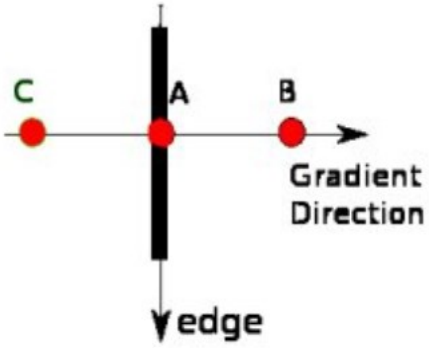

Fig. 10: Visualization of which points are considered

Point A is confronted with points B and C, which lay in the gradient direction. If A is greater than both, it is considered as a local point of maximum, otherwise it would be suppressed to 0.

The result is a Grayscale image, where the edges' color values are set to the gradient's local value.

Step 4: **Hysteresis Thresholding**

At this stage it is determined which of the edges identified at the previous point are significant and which are not.

To do so, two thresholds are defined: *maxVal* and *minVal*. Pixels with intensity gradient higher than *maxVal* are sure to be edges and pixels with intensity gradient below *minVal* are sure not to be edges.

Pixels whose intensity gradient falls in between these two values need to be classified as edges or non-edges based on their connectivity: if they are connected to "sure edge" pixels, they are considered to be part of edge; if else, they are suppressed to 0.

As an example, consider this case:

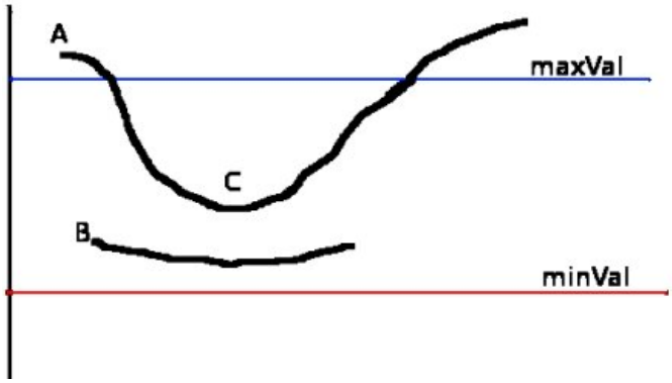

Fig. 11: Example for hysteresis thresholding

Both points B and C have an intensity gradient that falls in between *maxVal* and *minVal*, but only point C is considered to be part of an edge, as it is connected to point A, which is a sure edge as its intensity gradient is higher than *maxVal*.
In order to effectively recognize edges, the values chosen for these two thresholds are very important. A suggested way to define them is:

$$maxVal = 1{,}3 \cdot median \qquad minVal = 0{,}7 \cdot median$$

Points that are recognized as belonging to an edge are set to 255. The result is a Black and White image, where all the edges are thin white lines over a total black background.
This steps also removes small pixel noise, under the assumption that edges are long lines.

(opencv, s.d.)

After all these steps have been performed of the image of the sample, the result is the following:

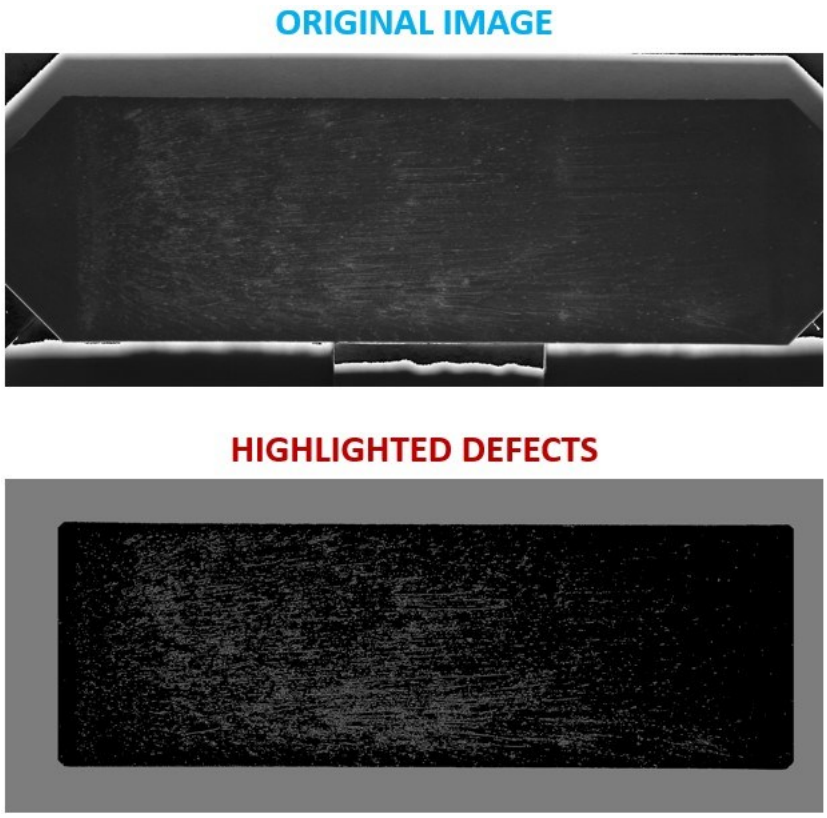

Fig. 12: Comparison of the original image with the post processed one

Defectiveness index

After the contours of the defects have been located in all the images, an index needs to be defined to represent how defective each sample's surface is.

Counting the amount of white pixels in each image is a first step, as the more defects are present, the bigger this number gets.
This method is not enough tough, because it has some flaws that make it clunky to work with and may even introduce some unwanted errors:

- the index so defined is of difficult interpretation, as the number of pixels is not correlated to anything. This means that it is quite difficult to tell whether the measured value is high or low, forcing to redefine the index interpretation every time an object with different dimensions is analyzed
- it does not take into account potential changes in the distance that separates the samples from the camera. Closer distances would be resulting in a higher number of white pixels, but this would only be attributed to the fact that the sample takes more space in the photo and its defects appear to be bigger
- it does not take into account for different camera resolutions, which acts on the measured index in a similar way as the previous issue

To solve the first problem, the defect index can be defined as the ratio of white pixels over the total number of pixels not covered by the mask. This results in a fraction from 0 to 1 that is very easy to interpret. It also gives a better representation of how defectiveness is perceived: comparing two samples with the same amount of defect edges(same amount of white pixels), where one has double the surface of the other, the one with the bigger surface will be classified as less defective.
Still, the issue regarding camera positioning and camera resolution is not addressed by this index.

A defectiveness index that addresses all the issues presented before can be found by replacing in the previous definition the total amount of pixels not masked (which can be interpreted as a measure of the surface area) with the length in pixels of a square whose pixel area is equal to that same amount of non-masked pixels. This makes even

more sense if considering the fact that the white pixels can be interpreted as the pixel length of all the defects' contours.

The ratio so defined, while being a bit less immediate to interpret, does not depend from the camera distance or the camera resolution, as long as these two factors are such that all the defects are clearly visible in the photos taken.

The defectiveness index is finally defined as:

$$l = \sqrt{N_{non-masked\ pixels}}$$

$$def\_ind = \frac{N_{white\ pixels}}{l}$$

PROs and CONs of Edge Detection

In literature regarding Surface Defects estimation, the most popular way to get an esteem of how defective a surface is can be summarized in three steps:

1) the defective area is blurred enough to represent the base color of the surface
2) the blurred image is subtracted from the original image, so that the defects are the only parts whose pixel colors are distant from 0
3) a dispersion index is calculated for the resulting image

More often than not, the dispersion index is the standard deviation of the color histogram of the final image, as in the article published by Jinsu Gim, Huaguang Yang, Lih-Sheng Turng already cited in the Introduction (Jinsu Gim, Huaguang Yang, Lih-Sheng Turng, 2023). The index so defined is easy to interpret: the more dispersed the final image is, the more defects should be present on the analyzed surface.
This does not take into account for the defects' color or the lighting conditions, tough. The same defect, but with a different color, would give variations in the grayscale color histogram that would result in a change in the standard deviation value; this effect can fictitiously increase or decrease the measured defectiveness, while the actual amount of defects has not been varied.
A similar problem arises when changing the type of light source: depending on it, the sample and the defects present on it can change color independently, thus changing the observed standard deviation.
Another issue is the fact that light does not necessarily reach every part of the surface in the same condition: source direction and intensity can change depending on the point considered on the surface.

The combination of the three effects just described lowers the repeatability of measurements taken with this method, as the setup required to take the photos has a very strict window inside which it can be varied to still obtain compatible results. This also means that an in-line production implementation of this method for quality control, while feasible, would be quite difficult and easily prone to faults.

The defective index defined using edge detection solves all these three problems, as it only checks for color gradients inside the image. This means that the measured index does not depend by lighting conditions or by the color perceived by the camera.
For these reasons, repeatability of the measurements is greatly increased: the measurements can be performed using any kind of light source and the color of the processed material can be changed without any worry that new experiments must be performed to characterize the surface defectiveness from zero. This also makes an hypothetical in-line quality control way easier to implement and robust.

On the other hand, edge detection has troubles when defects have different sizes relative to one another: elongated defects would have longer contours, meaning that they would be more represented than chunkier ones.
Edge detection also comes short when in need to classify different types of defects. If the run experiment requires a defect classification based on their color or their surface area, algorithms for these purposes must be implemented in addition to edge detection.

PROs	CONs
Not susceptible to lighting conditions	Elongated defects are more represented than chunky defects
Not too influenced by camera resolution	Can not classify defects by their color
Very easy to implement even with cheap setup	

Table 7: PROs and CONs of using edge detection for defectivenes estimation

RESULTS

After all the sample images have been processed, the results are collected in a table for further analysis.

n	Q_i [ccm/s]	p_b [bar]	T_m [°C]	t_d [min]	t_c [s]	def_ind
1	10	35	190	0	60	94,54
2	30	35	190	0	60	69,84
3	30	70	190	0	60	70,27
4	10	70	190	0	60	98,19
5	10	70	190	0	120	104,73
6	30	70	190	0	120	62,14
7	30	35	190	0	120	54,34
8	10	35	190	0	120	95,31
13	30	70	190	0	48	48,14
14	10	70	190	0	48	74,56
15	10	35	190	0	48	74,14
16	30	35	190	0	48	50,88
17	30	35	220	0	48	57,77
18	10	35	220	0	48	168,89
19	10	70	220	0	48	165,04
20	30	70	220	0	48	59,99
21	30	70	220	0	60	55,33
22	10	70	220	0	60	181,15
23	10	35	220	0	60	179,93
24	30	35	220	0	60	58,67
25	30	35	220	0	120	174,52
26	10	35	220	0	120	314,51
27	10	70	220	0	120	296,01
28	30	70	220	0	120	154,63
33	30	35	250	0	48	331,63
34	10	35	250	0	48	360,47
35	10	70	250	0	48	369,01
36	30	70	250	0	48	269,24
37	30	70	250	0	60	285,99
38	10	70	250	0	60	391,95
39	10	35	250	0	60	372,09
40	30	35	250	0	60	322,61
41	30	35	250	0	120	306,26
42	10	35	250	0	120	393,37
43	10	70	250	0	120	388,87
44	30	70	250	0	120	319,54

Table 8: Non-dried material measured Defective indices

n	Q_i [ccm/s]	p_b [bar]	T_m [°C]	t_d [min]	t_c [s]	def_ind
101	10	35	190	90	48	57,18
102	30	35	190	90	48	34,10
103	30	70	190	90	48	30,74
104	10	70	190	90	48	60,85
105	10	70	190	90	60	50,10
106	30	70	190	90	60	33,71
107	30	35	190	90	60	32,51
108	10	35	190	90	60	53,02
109	10	35	190	90	120	55,40
110	30	35	190	90	120	33,21
111	30	70	190	90	120	31,73
112	10	70	190	90	120	53,91
117	10	35	220	90	48	79,78
118	30	35	220	90	48	59,49
119	30	70	220	90	48	56,65
120	10	70	220	90	48	81,44
121	10	70	220	90	60	89,63
122	30	70	220	90	60	63,72
123	30	35	220	90	60	62,90
124	10	35	220	90	60	81,64
125	10	35	220	90	120	91,77
126	30	35	220	90	120	63,72
127	30	70	220	90	120	60,30
128	10	70	220	90	120	96,84
133	10	35	250	90	48	373,15
134	30	35	250	90	48	270,19
135	30	70	250	90	48	285,64
136	10	70	250	90	48	348,47
137	10	70	250	90	60	358,42
138	30	70	250	90	60	262,19
139	30	35	250	90	60	235,31
140	10	35	250	90	60	344,39
141	10	35	250	90	120	388,31
142	30	35	250	90	120	293,19
143	30	70	250	90	120	309,77
144	10	70	250	90	120	384,61

Table 9: Dried material measured Defective indices

Analysis of Variance

Given a hypothetical regression function, the *p-value* is the probability of obtaining the observed difference (or a greater one), given that the changed parameter has no influence on the outcome of the measured output (*Null hypothesis*). In other terms, it esteems the probability that changing only one input parameter, the measured output's variation is only to be attributed to noise introduced during sampling or during measuring phase.

As an example, if the *p-value* is 0.004, it means that there is a 0.4% chance that the observed difference is only caused by random noise that originates from sampling.

From a mathematical point of view, the *p-value* is determined by applying a Student's distribution (*T-distribution*) to the outputs corresponding to each of the two levels of an input parameter. This identifies the *Probability Density Functions* of each level, which can be represented as a curve in a bidimensional plane with the input parameter in the x-axis and the output parameter in the y-axis. The overlap area under the two curves is the probability that the measured output can be obtained independently from the chosen input parameter level. This area is called *probability value* or *p-value*.

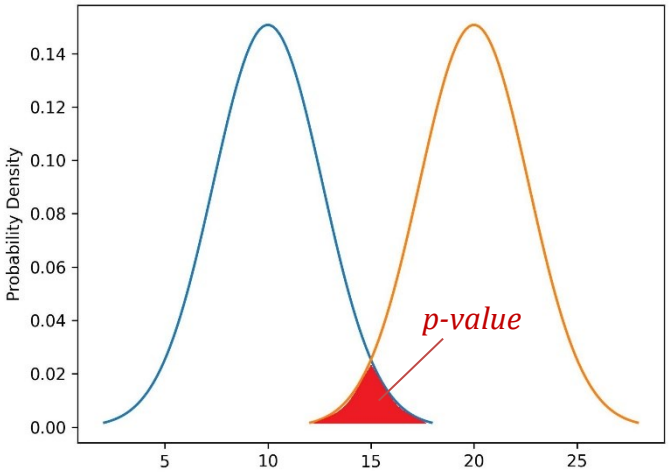

Fig. 13: p-value area

In case 3 or more levels are defined for a single parameter, the total dominion is divided into sub-dominions, each with extremes two successive levels of the input parameter.

Then, the previous definition can be applied to each sub-dominion, resulting in a different *p-value* for each one.

From the *p-value* table, obtained using the *Stat → ANOVA → General Linear Model → Fit General Linear Model* function with the Minitab software, it can be noticed that two parameters manifest very high *p-values*: Backpressure and Cycle time, just in the dominion between 48 and 60 s.

Assuming a significance level of 95%, the threshold value, over which a *p-value* is considered to be too high, is $\alpha = 0.05$. The two mentioned cases go well above this threshold, meaning that Backpressure and Cycle times under one minute have little to no influence on the observed Defects.

Coefficients

Term	Coef	SE Coef	T-Value	P-Value	VIF
Constant	159,8	11,3	14,17	0,000	
Q_i					
30	-61,13	7,98	-7,67	0,000	1,00
p_b					
70	-0,99	7,98	-0,12	0,902	1,00
T_m					
190	-55,45	9,77	-5,68	0,000	1,33
250	217,10	9,77	22,23	0,000	1,33
t_d					
90	-44,63	7,98	-5,60	0,000	1,00
t_c					
48	-3,36	9,77	-0,34	0,732	1,33
120	28,29	9,77	2,90	0,005	1,33

Table 10: p-value and standard deviation table

Principal Effects Plots

Principal Effects Plots are obtained by taking the mean of the outputs measured when an input parameter is kept fixed to one level. The points obtained are then reported in a bidimensional plane with the input parameter in the x-axis and the output parameter in the y-axis and connected with a straight line.

This allows for a better visualization of how much influence changing each parameter has on the response.

Injection Rate

Higher Injection Rates appear to be beneficial for Surface Defects reduction.

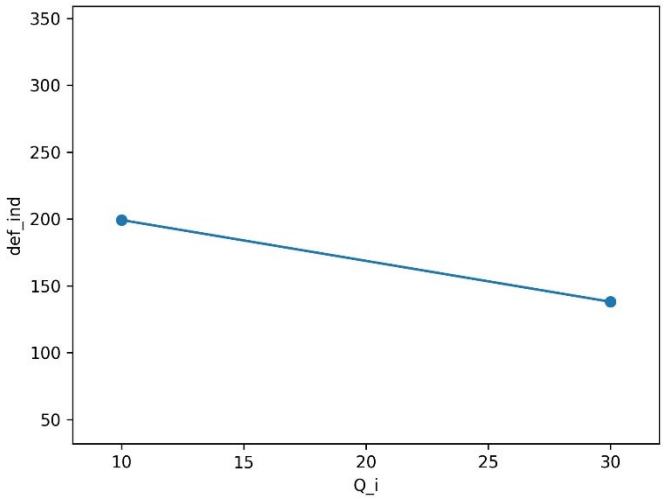

Fig. 14: Main Effect of Injection Flow Rate

To explain this effect, we need to look in literature at experiments where gas-counter pressure was applied and controlled during the injection phase to eliminate Surface Defects that were attributed to igroscopic retention of the processed material.
The idea behind these experiments was not to let water evaporate, which would have caused gaseous bubbles inside the mold that lead to defects. To achieve this goal, cavity pressure was controlled and kept above the saturation pressure of water until the melt was solidified.
Working with high Injection Rates may emulate this effect: the air present in the Mold before the injection would be expelled faster, but, as the air is a compressible fluid, (Yeong-Eun Yoo, Sang-Won Woo, Sun Kyoung Kim, 2012)

Backpressure

Changing Backpressure during the metering phase does not result in any meaningful changes in Surface Defects.

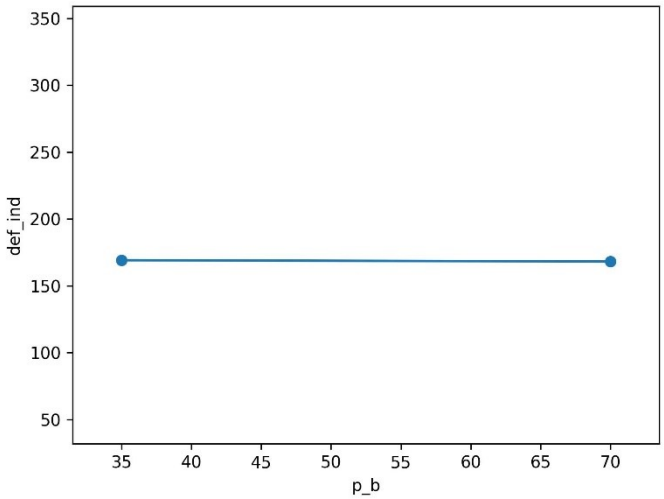

Fig. 15: Main Effect of Backpressure

The explanation for this can be found considering the way in which heat is added to the

plastic material to melt it. In an Injection Molding Machine, the provided heat can be attributed into two quotas:

a. *Frictional Heat*, which is the main contribution, representing around 70% of the total heat provided from the Machine to the plastic
b. *Thermal Heat*, provided by electrical resistances positioned around the cylinder body; these resistances are controlled by a PID controller and are not used as the main heat providers, but as precise regulators to achieve the desired Temperature

The fact that Backpressure has no influence on the output, even though in theory it should be resulting in more heat added to the plastic and consequently in higher defect occurrence, means that the regulation provided by the PID controller via the electrical resistances is enough to counterbalance the detrimental effects that raising Backpressure would have.

Melt Temperature

Melt Temperature is the most influent parameter on the Defect Index. Surface Defects are more present when Melt Temperature is high.

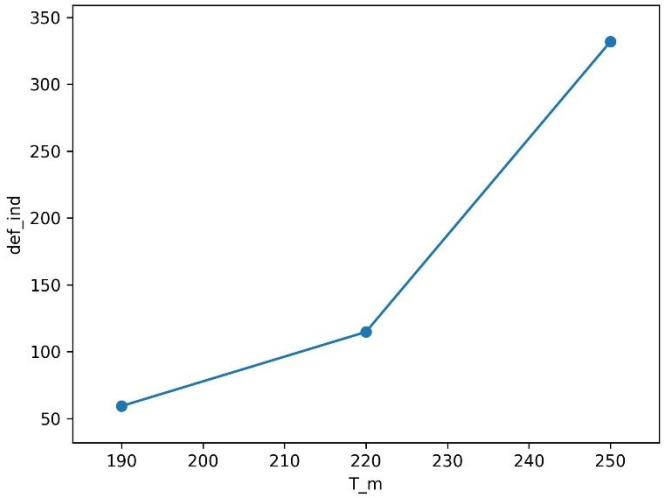

Fig. 16: Main Effect of Melt Temperature

In terms of Defect Index, the jump from 220 to 250 °C is much higher than the jump from 190 to 220 °C. To explain this, it can be hypothesized that the degradation of whatever additive is present in the recycled-PP can be considered as a thermically activated process. This means that the amount of material that gets degraded in a unit of time increases exponentially with Melt Temperature.

Noticeably, the influence of Melt Temperature on the Defect Index is so big that just reducing it may be able to completely negate the presence of Defects to the human eye, independently from the other processing parameters.
This is the case with all the samples that were obtained with Melt Temperature set to 190 °C: considered the human eye threshold to be *def_ind = 100*, it can be seen that all the samples obtained with this Temperature have lower Defect Index values.

Drying time

The material processed after having been dried for 90 minutes at 90 °C consistently shows lower Defect Index values.

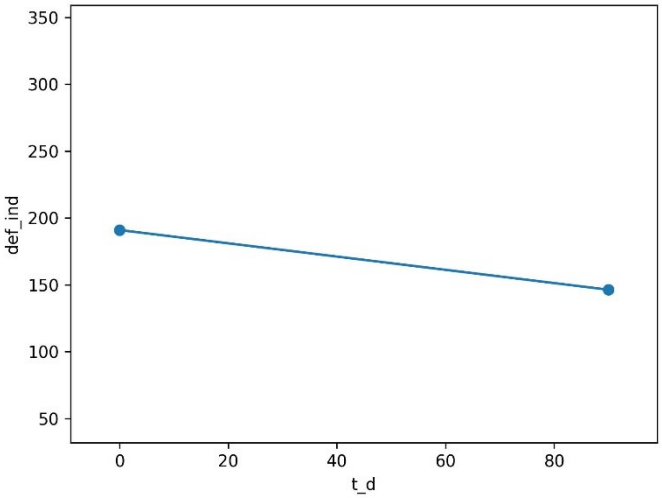

Fig. 17: Main Effect of Drying time

While virgin Polypropylene has very low water retention, the same can not be said for recycled Polypropylene. The additives present inside this material, introduced from the Mechanical Recycle process, show to have igroscopic behavior. This means that the material, as it was provided, had some water in it.
When the recycled-PP pellets are processed in the Cylinder, the water that was absorbed by the material gets turned into steam.
The steam behaves in the same way as the gases formed by additive degradation, meaning that it condenses onto the walls of the Mold while the Injection is happening. The drops of water that condense on the walls are dragged with the melt and determine Surface Defects that follow the flow lines.

Cycle Time

Higher Cycle times are connected to higher Defect Indices.

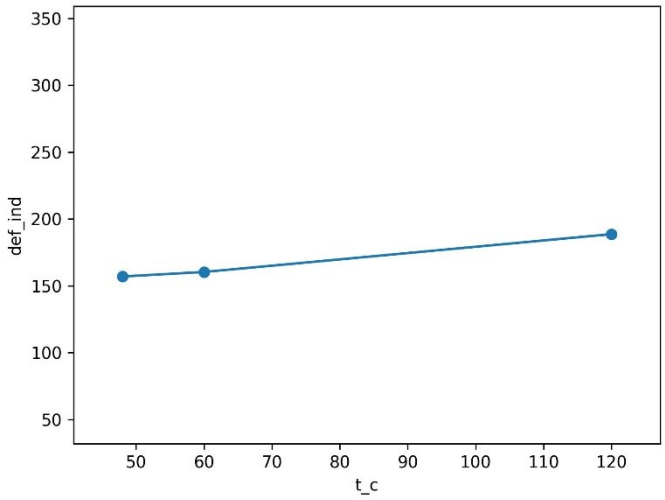

Fig. 18: Main Effect of Cycle time

Cycle time is used as a proxy for the time that the polymer spends at the preset Melt Temperature.
The molten polymer can be considered as a gas generator, which has a fixed gas generation rate for a certain Temperature and Drying condition. If this fluid is kept at the same Temperature for a certain amount of time, the ingenerated gas increases linearly with the amount of time spent in these conditions. This hypothesis finds enough support in the main effect plot for Cycle time, as the 3 points located for the 3 predetermined levels lie with sufficient accuracy on the same straight line.

The fact that the *p-value* for the lower range is very high, meaning that Cycle time has less weight on the output in this range, can be attributed to the fact that the difference between the two extremes of this range is not that high. This low difference, combined with the fact that the average gas generation rate is not that high, results in low statistical meaning of this parameter in that range.
Even tough it has low statistical weight, the difference in the outputs for these two levels can still be measured and used to support the linear dependence hypothesis.

Interaction Plots

While Main Effects Plots were obtained by taking the mean of all the outputs measured for every level of an input parameter, Interaction Effects Plots are obtained in the same way, but considering only the outputs obtained with a fixed value of a second input parameter.

The points located in this way are drawn in the same bidimensional planes of the Main Effects. Then, all the points for which the second input parameter is the same are linked together by straight segments, in ascending order.

If the straight segments between two levels of the first input parameter have different steepness, it means that the two input parameters that have been considered are interacting together in that range.

As already observed while analyzing the statistical significance of the parameters and the Main Effects, Backpressure does not influence in any way the monitored output. This is manifest with the Interaction Plots too, as all the plots that use Backpressure as one of the two input parameters contain segments that have the same exact steepness inside the same range.

Of the remaining input parameters, the only pairing between which there seems to be no interaction is the pair *Flow Rate – Cycle Time*. All the other pairs appear to have some sort of interaction.

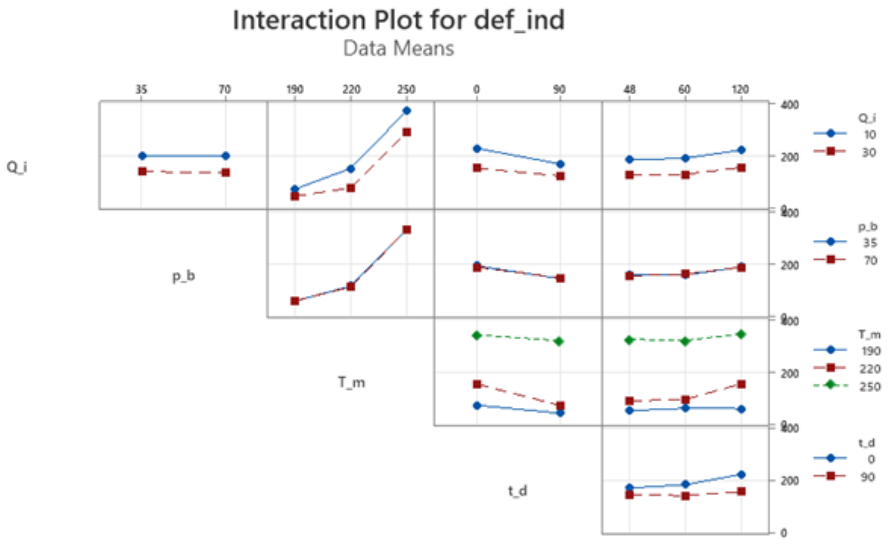

Fig. 19: Interaction plots overview

Flow Rate vs Melt Temperature

In the lower Temperature range (190 – 220 °C), increasing the Melt Temperature makes the improvement that comes from higher Flow Rates get better.
The same does not happen in the higher Temperature range, where the two factors show no interaction.

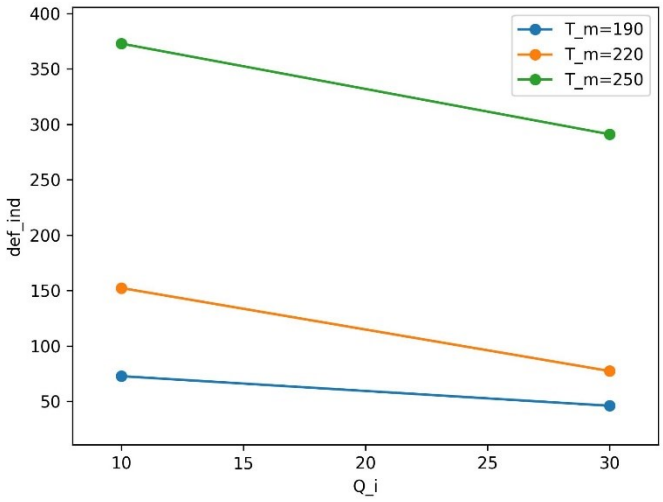

Fig. 20: Interaction between Flow Rate and Melt Temperature

It is very difficult to imagine how the Melt Temperature should be influencing the way the air present inside the mold gets compressed by changing Flow Rate, especially because the Injection Phase happens very fast, so the Thermal exchange between air and polymer is negligible.
Thus, it is more probable that the interaction registered at low Temperatures needs to be attributed to the fact that the Surface Defect Index *def_ind* has a floor value, corresponding to a Surface that has the lowest possible amount of defect and below which it is not feasible to go.

Flow Rate vs Drying time

For material that was previously dried it is less beneficial to use higher Injection Rates.

While it can be said that more *def_ind* values close to the floor level are present in the group of samples that

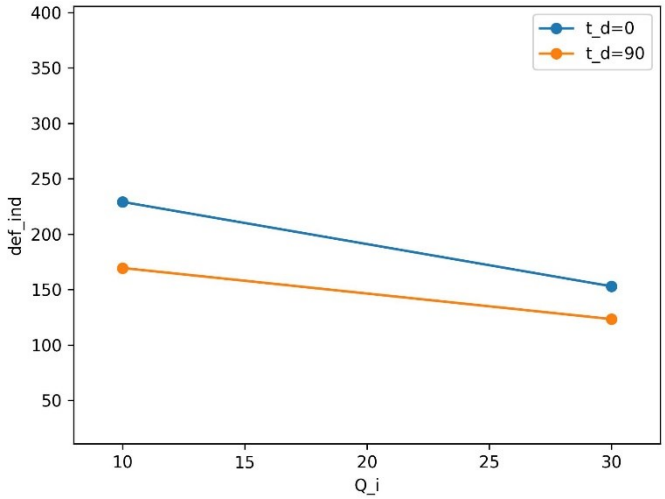

Fig. 21: Interaction between Flow Rate and Drying time

was previously dried, the main reason for this difference might be another one.

The steam present in the processed material tends to emerge from the liquid polymer and diffuse in the air present inside the mold cavity. This process happens fast enough to be relevant during the Injection Phase and contributes in raising the gas-counterpressure ahead of the Injected fluid: the steam present in the liquid diffuses in the air, both raising the resulting gaseous mixture Temperature and the amount of gaseous mass present in the same volume; these two effects compound and result in higher gas-counterpressure ahead of the fluid than the counterpressure that would result if no water was present in the processed material.

Injection Rate vs Cycle time

As previously stated, there is no interaction between these two parameters.

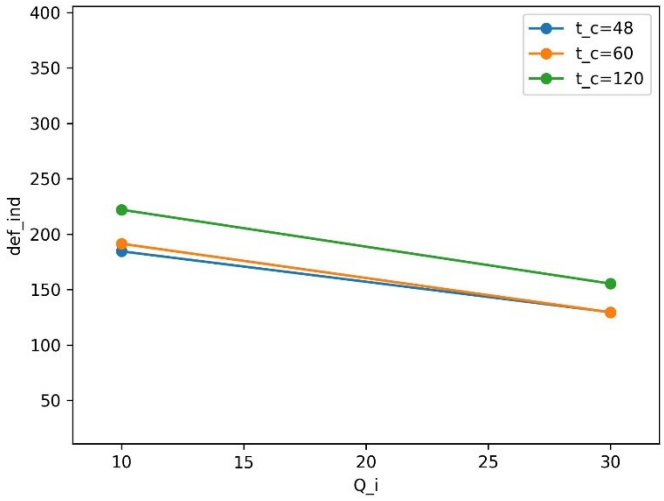

Fig. 22: Interaction between Flow Rate and Cycle time

While Longer Cycle times would mean that more degradation gas would be present in the injected fluid, the fact that there is no statistically relevant difference in Injection Rate's influence over the output must mean that all the additives present in the recycled-Polypropylene that can be thermically degraded have already been turned into gas after the minimum processing time has passed.

Melt Temperature vs Drying time

In the lower Temperature range, the non-dried material is more severely affected from a Temperature increase. The opposite is true in the Higher Temperature range.

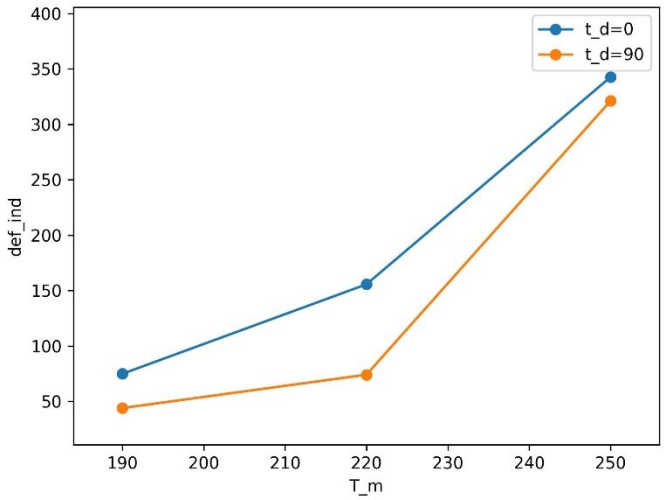

Fig. 23: Interaction between Melt Temperature and Drying time

Let's consider only the plot obtained for *t_d = 90*. The way in which the points are disposed clearly hints to the fact that the additives degradation is a thermically activated process, as the jump from 220 to 250 °C is around 20 times bigger than the jump from 190 to 220 °C.
The *def_ind* value read at 190 °C in this condition almost coincides with the lowest possible value obtainable for this parameter

According to the hypothesis that $T_m = f(def\_ind)$ is an exponential function, the difference between the plots obtained for the two conditions of t_d should be an horizontal or an ascending straight line. This is not the case, as the outputs obtained at the highest Temperature show convergence of the two lines while rising Melt Temperature.
To explain this behavior, we follow the same reasoning that was used to explain the convergence at low Temperature: once again we must make the assumption that there is an upper bound that limits the possible value of the parameter *def_ind*, which, from the collected data, seems to be identifiable as $def\_ind_{max} \approx 400$.
This is easy to understand when thinking about an hypothetical worst case limit situation, in which the processing conditions are so bad that the sample alternates a line of base color to a line of defective color: in this situation, half of the surface is considered Defect and there is no way to increase this fraction, so it is considered to be the upper limit for defectiveness in the ideal case. Once the non-ideal nature of the

process is considered and after a translation of this concept to *def_ind*, the natural upper bound to the Defectiveness Index is defined.

Melt Temperature vs Cycle time

In the lower Cycle time range (48 – 60 s) there is no significant interaction between Melt Temperature and Cycle Time.

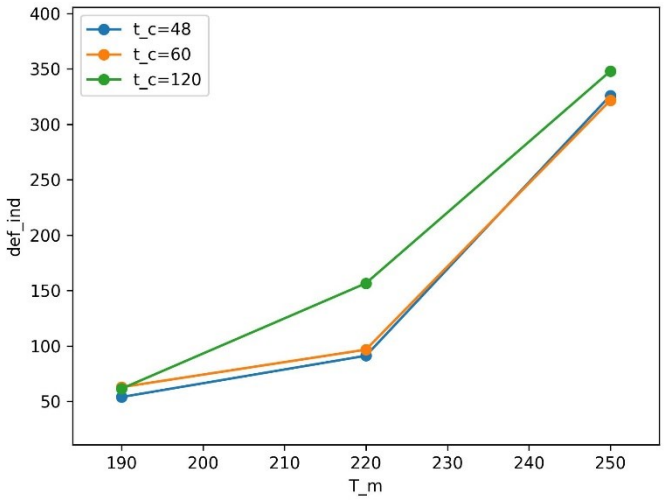

Fig. 24: Interaction between Melt Temperature and Cycle time

In the upper range, instead, the two plots start from the same point for 190 °C, but the one with higher Cycle time increases more quickly in the first half of the dominion. In the second half, from 220 to 250 °C, the plots show a convergence similar to the previous case, which can be explained in the same way.

Cycle time vs Drying time

While for the humid material increasing Cycle time is detrimental for the Surface Defects, the dried material does not show to be very affected by the amount of time spent at high Temperature.

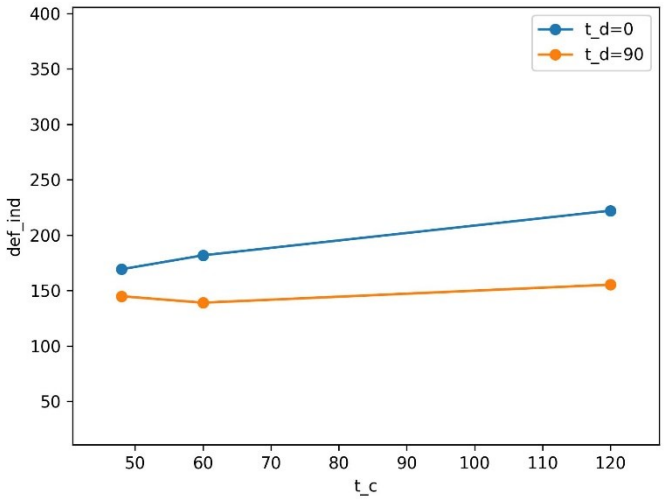

Fig. 25: Interaction between Cycle time and Drying time

As previously noted when discussing *Injection Rate vs Drying time*, this means that

the additives responsible for Surface Defects are very quick to degrade into gas, so their influence on the output is already at its maximum at the lower Cycle time value and cannot be changed increasing this parameter.

On the other hand, the fact that the humid material presents an increase in Surface Defectiveness for higher Cycle times must mean that the water present in the material as igroscopic retention is gradually released over time at a more or less constant rate.

Linear Regression Model

After the most influent parameters and their interactions have been identified, a Linear Model can be created applying a linear regression to the measured data. To create this model the *LinearRegression* class from the python *scikit-learn* library was used.

Preprocessing (parameters normalization)

Before proceeding with the model creation, it is recommended to normalize the input parameters remapping the lower level to 0 and the higher level to 1. The formula for this is:

$$x = \frac{X - X_L}{X_H - X_L}$$

This normalization ensures that the interactions between multiple parameters are also bounded to vary in a range from 0 to 1.
In this way, every parameter variation is considered equal and the coefficient corresponding to that parameter represents how influential it is in determining the output value.
In other words: the parameters whose coefficient have the highest absolute value are the more influential ones, while smaller coefficients mean that that parameter is less influent.

The normalization makes so that the created regression model is easy to read and exposes immediately how much certain parameters need to be changed to obtain a desired change in the output.

Final formulation of the Regression Model

The general formulation of a Linear Regression Model with first order interactions is:

$$def\_ind = (c_1 \cdot Q_i + c_2 \cdot p_b + c_3 \cdot T_m + c_4 \cdot t_d + c_5 \cdot t_c) + cost + \sum_{i \neq j} c_{ij} \cdot par_i \cdot par_j$$

For the final formulation of the regression model, only the most relevant parameters and interactions need to be taken into consideration. This reduces its formula to:

$$def\_ind = (c_1 \cdot Q_i + c_3 \cdot T_m + c_4 \cdot t_d + c_5 \cdot t_c) + (c_{13} \cdot Q_i T_m + c_{14} \cdot Q_i t_d + c_{34} \cdot T_m t_d + c_{35} \cdot T_m t_c + c_{45} \cdot t_d t_c) + cost$$

As Melt Temperature and Cycle Time are varied over 3 levels, two different dominions as defined for each of these parameters; this means that a different regression shall be applied in the two different regions, meaning that 2 x 2 = 4 different regression models shall be used (one for each combination of the dominions).

The coefficients and the regression scores obtained for each regression models are reported in the following tables.

Low T_m, low t_c:

Q_i	T_m	t_d	t_c	Q_i x T_m	Q_i x t_d	T_m x t_d	T_m x t_c	t_d x t_c	cost
-48,16	67,54	-46,31	15,29	-45,07	48,22	-15,40	-3,46	-12,69	89,00

Table 11: Regression coefficients for low Melt Temperature and low Cycle time

Regression score	0,912

High T_m, low t_c:

Q_i	T_m	t_d	t_c	Q_i x T_m	Q_i x t_d	T_m x t_d	T_m x t_c	t_d x t_c	cost
-87,03	233,34	-54,20	13,13	-12,77	35,81	15,79	-9,85	-15,29	152,79

Table 12: Regression coefficients for high Melt Temperature and low Cycle time

Regression score	0,977

Low T_m, high t_c:

Q_i	T_m	t_d	t_c	Q_i x T_m	Q_i x t_d	T_m x t_d	T_m x t_c	t_d x t_c	cost
-56,81	91,27	-41,07	25,36	-52,53	59,27	-62,31	61,34	-53,58	96,89

Table 13: Regression coefficients for low Melt Temperature and high Cycle time

Regression score	0,919

High T_m, high t_c:

Q_i	T_m	t_d	t_c	Q_i x T_m	Q_i x t_d	T_m x t_d	T_m x t_c	t_d x t_c	cost
-101,95	190,61	-103,41	79,27	-6,18	44,48	74,97	-33,55	-38,71	188,18

Table 14: Regression coefficients for high Melt Temperature and high Cycle time

Regression score	0,958

Model test

To test the effectiveness of the created Linear Model, a series of experiments was conducted with different processing parameters to the ones used to create the model. The results are reported in four tables.

Low T_m, low t_c:

n	Q_i [ccm/s]	p_b [bar]	T_m [°C]	t_d [min]	t_c [s]	def_ind	predicted	delta	delta %
50	10	35	205	0	60	90	136,34	46,34	51,49
51	10	60	205	0	60	79,79	136,34	56,54	70,87
52	10	50	205	0	48	79,49	122,77	43,29	54,46
53	25	50	205	0	48	40,66	69,75	29,09	71,56
54	30	70	205	0	48	49,33	52,08	2,75	5,57
58	15	35	205	0	60	54,07	118,66	64,59	119,46
150	10	35	205	90	60	95,45	69,64	-25,8	-27,04
151	10	60	205	90	60	103,77	69,64	-34,13	-32,89
152	10	50	205	90	48	100,7	68,77	-31,93	-31,71
153	25	50	205	90	48	56,9	51,91	-4,99	-8,78
154	30	70	205	90	48	50,14	46,29	-3,85	-7,67
158	15	35	205	90	60	61,25	64,02	2,77	4,53

Table 15: Predicted def_ind values for low Melt Temperature and low Cycle time

High T_m, low t_c:

n	Q_i [ccm/s]	p_b [bar]	T_m [°C]	t_d [min]	t_c [s]	def_ind	predicted	delta	delta %
60	10	35	235	0	60	290,4	277,67	-12,73	-4,38
61	10	60	235	0	60	280,35	277,67	-2,68	-0,96
62	10	50	235	0	48	282,57	269,46	-13,11	-4,64
63	25	50	235	0	48	180,87	199,4	18,54	10,25
64	30	70	235	0	48	164,92	176,05	11,13	6,75
68	15	35	235	0	60	172,73	254,32	81,59	47,24
160	10	35	235	90	60	135,36	216,08	80,72	59,64
161	10	60	235	90	60	197,59	216,08	18,48	9,35
162	10	50	235	90	48	249,42	223,15	-26,26	-10,53
163	25	50	235	90	48	178,91	179,95	1,04	0,58
164	30	70	235	90	48	138,13	165,55	27,42	19,85
168	15	35	235	90	60	179,87	201,68	21,8	12,12

Table 16: Predicted def_ind values for high Melt Temperature and low Cycle time

Low T_m, high t_c:

n	Q_i [ccm/s]	p_b [bar]	T_m [°C]	t_d [min]	t_c [s]	def_ind	predicted	delta	delta %
50	10	35	205	0	60	90	142,53	52,53	58,37
51	10	60	205	0	60	79,79	142,53	62,74	78,63
55	25	70	205	0	120	60,79	136,25	75,46	124,13
56	25	35	205	0	120	50,6	136,25	85,66	169,29
57	15	35	205	0	120	62,68	177,79	115,12	183,66
58	15	35	205	0	60	54,07	121,76	67,69	125,19
150	10	35	205	90	60	95,45	70,31	-25,14	-26,34
151	10	60	205	90	60	103,77	70,31	-33,47	-32,25
155	25	70	205	90	120	85,28	54,91	-30,38	-35,62
156	25	35	205	90	120	51,24	54,91	3,66	7,15
157	15	35	205	90	120	79,28	66,81	-12,47	-15,73
158	15	35	205	90	60	61,25	64,36	3,11	5,07

Table 17: Predicted def_ind values for low Melt Temperature and high Cycle time

High T_m, high t_c:

n	Q_i [ccm/s]	p_b [bar]	T_m [°C]	t_d [min]	t_c [s]	def_ind	predicted	delta	delta %
60	10	35	235	0	60	290,4	283,49	-6,91	-2,38
61	10	60	235	0	60	280,35	283,49	3,13	1,12
65	25	70	235	0	120	289,07	267,2	-21,87	-7,57
66	25	35	235	0	120	297,65	267,2	-30,45	-10,23
67	15	35	235	0	120	331,45	319,72	-11,73	-3,54
68	15	35	235	0	60	172,73	257,22	84,5	48,92
160	10	35	235	90	60	135,36	217,56	82,2	60,73
161	10	60	235	90	60	197,59	217,56	19,96	10,1
165	25	70	235	90	120	273,1	195,92	-77,18	-28,26
166	25	35	235	90	120	271,6	195,92	-75,67	-27,86
167	15	35	235	90	120	293,3	226,21	-67,09	-22,87
168	15	35	235	90	60	179,87	202,41	22,54	12,53

Table 18: Predicted def_ind values for high Melt Temperature and high Cycle time

The defective indices for the samples obtained at higher Melting Temperature can be predicted somewhat accurately by the Linear Regression model, while the ones obtained at lower Melting Temperature are overestimated by a lot.

This observation adds further credibility to the hypothesis that the degradation the additives present in the recycled-PP can be considered as a thermically activated process: when comparing an exponential function (representing a thermically activated process) to a linear function, both defined between two points *H* and *L*, it can be observed that in the exponential function is always below the linear one. At low Temperatures, when the degradation process has just started, the exponential function increases at very slow pace, so the predicted values using a linear function will always be overestimating the true value by a lot.

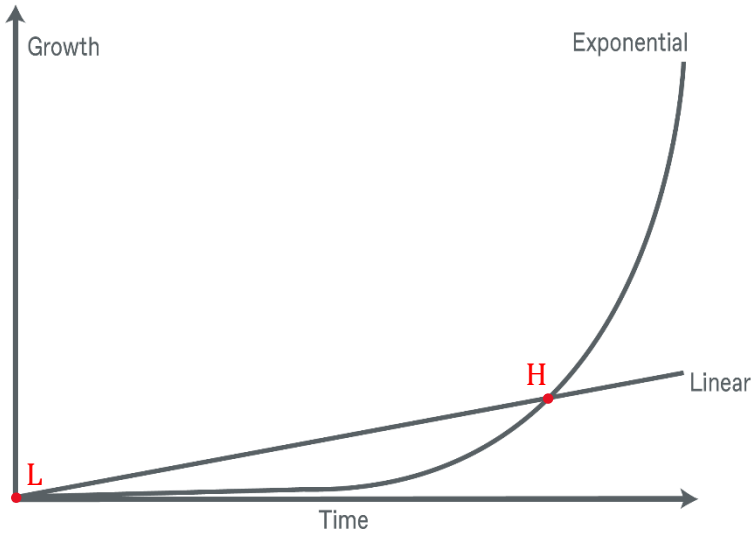

Fig. 26: comparison of exponential vs linear increase between two points

One more trend that can be observed in this dataset is the tendency to overestimate when the material is not dried and underestimate in the other case.
Once again, taking for good that the exponential function could represent the correct interpolation choice, this would mean that the exponent of the exponential function changes in response to the processed material being dried or not.

Mold Contamination

While working with recycled-PP pellets, it was noticed that on the mold used there kept forming a layer of dirt. As this only happened with this kind of material, it was hypothesized that the cause of Surface Defects and Mold Contamination was the same.

Then, we wanted to figure out whether the conditions that lead to higher Surface Defects were linked to the conditions that lead to higher contamination of the Mold's walls.

To further investigate mold contamination and the conditions that lead to more dirt deposits, it was scheduled a visit to FHP establishment in Monselice.

Fig. 27: Photo of the FHP establishment in Monselice

In this establishment the main production consists of drying racks, both plastic ones and metallic ones. Recently they started the production of some components made of post-consumer recycled Polypropylene. Since then, the main issue that rose has been that their Molds get very dirty very quickly.

These layers of dirt force the interruption of production, as the mold shape is replicated with less accuracy the more the dirt deposits on the Mold's walls.

After much time spent producing parts with this material, some signs started to be spotted that could indicate corrosion caused from the contamination.

Analyzed Molds presentation

Dinamity Leg Joint

LEAST prone to contamination

Coated: Yes

Heat Chamber: Yes

Injection Point: direct

Screw Diameter: 60 mm

Metering Run: 270 mm

Injected Volume: 763 cm^3

Injection Temperature: 230°C

Medium Mold Temperature: 25°C

Cycle time: 39 s

Flow Rate: 7 g/s

Fig. 28: Dinamity leg joint photo

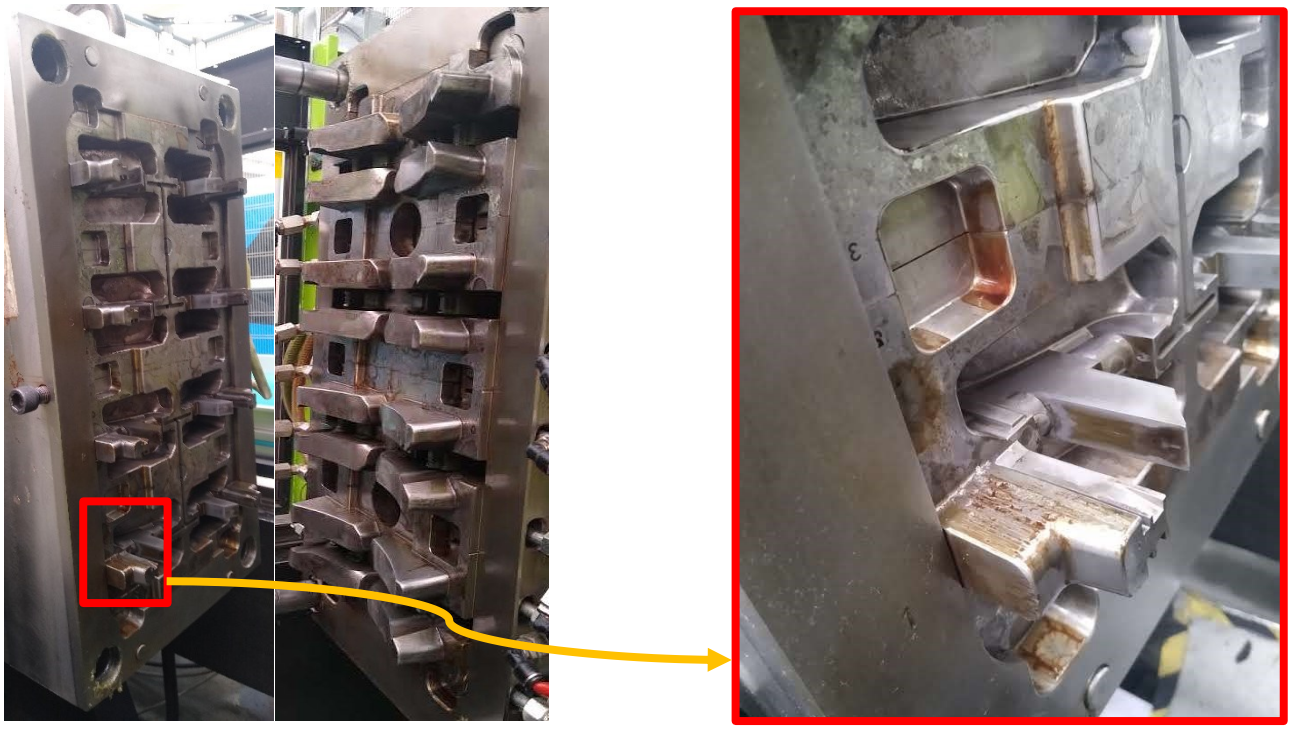

Fig. 29: Dinamity leg joint's mold, with zoom on some layers of dirt deposited on its walls

This Machine gave no visible surface defects on the formed pieces while automatically cycling, but surface defects came to be after a few minutes stop.
No blowholes are present to allow for a better exit to the air present in the cavity, so all the air and the gases must be expelled alongside the contour of the piece present in the divisor plane of the two mold pieces.

Bridge Corner

prone to contamination
Coated: Yes
Heat Chamber: No
Injection Point: submerged (injection point under the divisor plane of the Mold)
Screw Diameter: 55 mm
Metering Run: 210 mm
Injected Volume: 500 cm^3
Injection Temperature: 230°C
Medium Mold Temperature: 37°C
Cycle time: 25 s
Flow Rate: 6,4 g/s

Fig. 30: Bridge corner photo

Fig. 31: Bridge corner's mold

As for the former Machine, here too there were no visible surface defects on the formed pieces while automatically cycling, but came to be after a few minutes stop.

As no blowholes are present to allow for a better exit to the air present in the cavity, here too the air and gases must be expelled alongside the contour of the piece present in the divisor plane of the two mold pieces.

Dinamik Ring-Cover

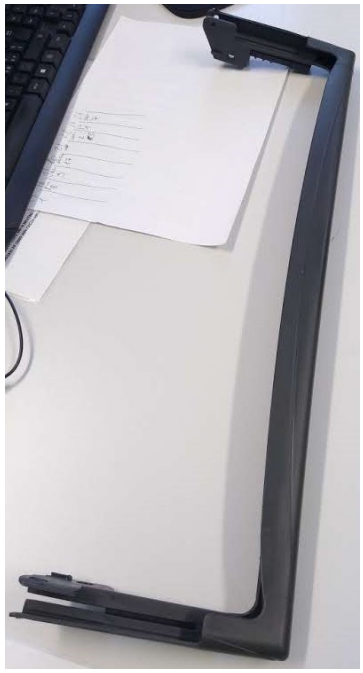

Fig. 32: Dinamik ring cover photo

MOST Prone to contamination

Coated: No

Heat Chamber: Yes

Injection Point: submerged (injection point under the divisor plane of the Mold)

Screw Diameter: 105 mm

Metering Run: 390 mm

Injected Volume: 3380 cm^3

Injection Temperature: 230°C

Medium Mold Temperature: 45°C

Cycle time: 45 s

Flow Rate: 8,5 g/s

Fig. 33: Dinamik ring cover's mold

This Injection Molding Machine produced pieces with no surface defects while cycling and, even after a few minutes stop, surface defects were very hard to see, if there were any.
Similarly to the previous molds, the air and gases inside the cavity are expelled from the shape's contour alongside the divisor plane of the two mold pieces.

Considerations on Contamination

In the examined cases, the highest contamination manifested with the machine that had the highest throughput time, decreasing the less time was spent by the material at high Temperature inside the Cylinder.

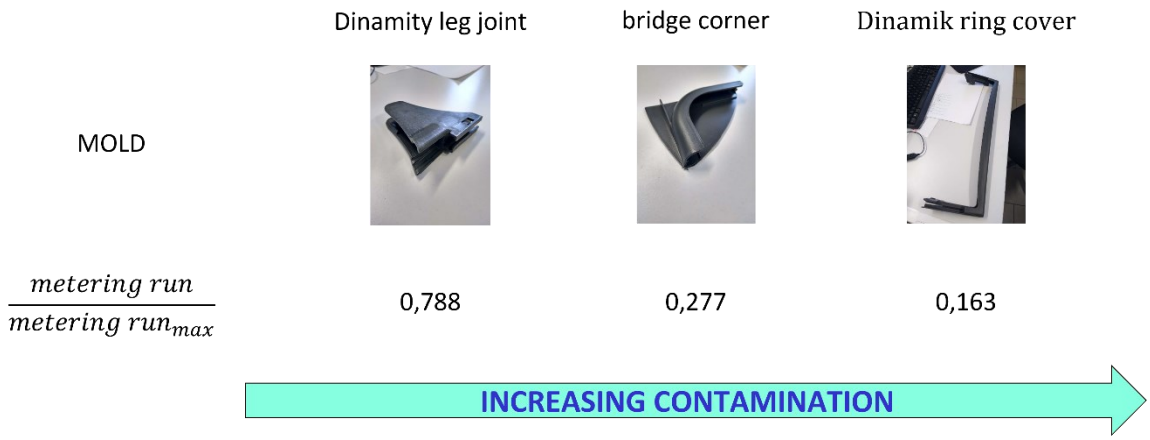

Fig. 34: correlation between mold contamination and fraction of the maximum metering run used

This resembles the results obtained in laboratory for the surface defectiveness: at equal conditions for Melt Temperature, Drying time and Injection Flow Rate, the material that determines the highest surface defectiveness is the one that has spent more time at high Temperature inside the Cylinder.
For this reason, it can be stated that the root cause of the problems is the same, and it can be identified in how much of the additives present in the recycled material is degraded before the injection inside the cavity.

Other factors that need to be taken into consideration are that a higher contamination rate manifested when there was no chemical coating on the Mold's surface and Mold geometry.

It can be hypothesized that the chemical coat transformed the mold's surface in a way that would lower the chance to have nucleation points for the condensation of gases. This would result in a reduction of contamination.
Regarding Mold geometry, the Molds that offer less resistance to gas expulsions give less time to the degraded material to deposit on the Mold's walls, resulting in lower contamination rates.

Finally, Medium Mold Temperature can be considered as concurring to dirt deposit, as lower Temperatures mean a greater Temperature gradient between gas condensation point and wall Temperature. This would lead to faster condensation.

Considerations on Surface defects

Before processing, all Recycled Polypropylene pellets were thermically treated for 90 minutes at 90°C to remove any water present in it in the form of igroscopic retention.
All the Injection Machines had same Melt Temperature of around 235°C and comparable Injection Rates.
When artificially augmenting Residence time by waiting for 3 minutes before injecting the material, the only outlier was the Dinamik Ring-Cover, as with this mold surface defects were not significant even for very high Residence times. This may be attributed to the particular conformation of the cavity: the bigger space would allow for a faster gas expansion, as its partial pressure (which drives gas expansion through the air) would increase more slowly; as a consequence, the gas would diffuse more in the air instead of stagnating on the wall front (where it would condense and determine defects).

Further o*bservations*

Contamination and Surface Defects seem to be related to the same root cause (which is presence of additive material inside recycled-PP). The dynamics that lead to their manifestation must be different. For Contamination, it's a matter of how much gas

condenses on the Mold's walls during all the process, while for Surface Defects it's a matter of creating conditions for the gas to condense just in the injection phase.

As for Surface Defects, their manifestation can be limited also by artificially rising gas counter pressure inside the cavity, so that the gas present inside the molten polymer wouldn't even be able to surface during injection.
This, while contrasting effectively Surface Defects, does nothing to decrease the contamination rate on the surface of the Mold.
Taken this in consideration, presence of Surface Defects surely leads to Contamination, but eliminating them is not enough to guarantee absence of deposit.
Noticeably, during production Surface Defects didn't appear even though Flow Rates were small and Injection Temperatures were high compared to the experiments conducted in laboratory. Even though these two effects should be detrimental for Surface Defects, the very low Cycle time means that the recycled polymer has a smaller window of time to degrade and this could counter balance the detrimental effects.
Other thing that may be reducing Surface Defects could be the more elaborate geometry of the produced pieces, as even in laboratory was noted that when Injection Molding more elaborate geometries (like a cup for automotive), the more convoluted path for the molten polymer meant that the pieces were more resilient to this kind of defect.

Conclusions

A novel method to evaluate surface defectiveness for injection molded objects was developed. This method, when compared to other methods present in literature, is easier to implement and is more robust with respect to changing light conditions. On top of increasing the repeatability of the experiments, this method would be easier to implement for quality control checks on in-line industrial production.

From the analysis of the collected data, it was reconstructed how each processing parameter influences the defectiveness of the injection molded samples. A Linear Regression Model was built and then tested on samples obtained in different conditions to the ones described in the Multifactorial Design of Experiment. Checking the correspondence between predicted values from this model and the defectiveness indices measured from the photos of the test samples, further information on this material behavior was obtained.

The most influential factor is Melt Temperature: if it is possible to lower it, doing so can completely solve the surface defectiveness issue. The more the Melt Temperature is risen, the faster the defectiveness increases, meaning that the effect of this parameter on surface defectiveness is more than linear. Having a high Melt Temperature means that the processes that cause the additive present in the material to degrade are accelerated, thus increasing the defects caused by their degradation.

Drying the pellets before processing them reduces the amount of defects, but they are still significatively present. This means that the igroscopic retention, while being a contributing factor to surface defects, is not the only one. This confirms that there must be some additives present in the material that degrade at high Temperatures to form gases.

Increasing Cycle time or Residence time resulted in an increase on the defectiveness index, meaning that the material degradation does not happen all at once: the more the material is kept at high Temperature, the more material will degrade. This effect is

well represented by a linear function, meaning that the degradation rate is constant with respect to time.

Increasing Injection Flow Rate resulted in lower surface defectiveness. The reason to this seems to be that higher injection rates create a fictitious gas counter-pressure inside the mold cavity, which prevents the gases inside the molten polymer to emerge to the surface during the injection.

Changing Backpressure had no statistically observable influence over surface quality. Although higher Backpressure means higher shear stress to melt the polymer, which would cause more heat to be transferred to the fluid, the effects in this supposed change were not seen. The reason for this is to be attributed to the PID controller that monitors the Cylinder Temperature, indirectly monitoring the polymer Temperature too: if the shear stress applied to the material acts in a way to increase its Temperature, the sensors inside the Cylinder read this change and the PID controller answers to that by lowering the amount of heat contributed by the resistances present in the machine. This feedback-based control system is sensible enough to compensate for the excess of heat that is provided by the increase in shear stress.

Finally, when considering how processing conditions have effect over Contamination of the Mold walls, it was observed that keeping the recycled-PP at high Temperature for longer times resulted in an increase in contamination rates. This indicates that the very same degradation that is responsible for the increase in surface defectiveness even after the material has been dried, is also responsible for the dirt layers that get deposited onto the mold's walls. The gases produced from the additives present in the recycled polypropylene condense on the mold, and the conditions that favor material deterioration are also the ones that lead to a faster contamination of the mold used.

References

AshaiKASEIplastics. (2018). *polypropylene_processing_guide.* Retrieved from akplastics.com: https://www.akplastics.com/wp-content/uploads/2020/06/asahikasei_polypropyleneprocessingguide_2018_0.pdf

Dian Rong, Xiuqin Rao, Yibin Ying. (2017). Computer vision detection of surface defect on oranges by means of a sliding comparison window local segmentation algorithm. *Computers and Electronics in Agriculture*, 59-68. doi:https://doi.org/10.1016/j.compag.2017.02.027

DrugPlastics. (2022, 03 18). *An Introduction to Advanced Plastic Recycling*. Retrieved from drugplastics.com: https://www.drugplastics.com/an-introduction-to-advanced-plastic-recycling/

Jiahuan Liu, Fei Guo, Huang Gao, Maoyuan Li, Yun Zhang, Huamin Zhou. (2021). Journal of Manufacturing Processes 70 (2021) 400–413. *Journal of Manufacturing Processes*, 400-413. doi:https://doi.org/10.1016/j.jmapro.2021.08.034

Jian Wang, Qianchao Mao, Nannan Jiang, Jinnan Chen. (2021). Effects of Injection Molding Parameters on Properties of Insert-Injection Molded Polypropylene Single-Polymer Composite. *Polymers*. doi:https://www.mdpi.com/1417262

Jinsu Gim, Huaguang Yang, Lih-Sheng Turng. (2023). Transfer learning of machine learning models for multi-objective process optimization of a transferred mold to ensure efficient and robust injection molding of high surface quality parts. *Journal of Manufacturing Processes*, 11-24. doi:https://doi.org/10.1016/j.jmapro.2022.12.055

Jinsu Gim, Lih-Sheng Turng. (2022). A review of current advancements in high surface quality injection molding. *Polymer Testing*. doi:https://doi.org/10.1016/j.polymertesting.2022.107718

Jinsu Gim, Lih-Sheng Turng. (2022). A review of current advancements in high surface quality injection molding: Measurement, influencing factors, prediction, and control. *Polymer Testing*. doi:https://doi.org/10.1016/j.polymertesting.2022.107718

KBdelta. (n.d.). *The Importance of Injection Speed of an Injection Molding Machine*. Retrieved from kbdelta.com: https://kbdelta.com/blog/importance-injection-speed-injection-molding-machine.html

Marielle E. H. Creusen, Jan P. L. Schoormans. (2005). The Different Roles of Product Appearance in Consumer Choice. *The Journal of Product Innovation Management*. doi:https://doi.org/10.1111/j.0737-6782.2005.00103.x

MathWorks. (n.d.). *Types of Morphological Operations*. Retrieved from mathworks.com: https://it.mathworks.com/help/images/morphological-dilation-and-erosion.html

opencv. (n.d.). *Canny Edge Detection*. Retrieved from opencv.org: https://docs.opencv.org/4.x/da/d22/tutorial_py_canny.html

Payman Moallem, Navid Razmjooy, Mohsen Ashourian. (2013). Computer vision-based potato defect detection using neural networks and support vector machine. *International Journal of Robotics and Automation* . doi:http://dx.doi.org/10.2316/Journal.206.2013.2.206-3746

PlasticsEurope. (n.d.). Recycling technologies. *PlasticsEurope*.

Qingzhong Li, Maohua Wang, Weikang Gu. (2002). Computer vision based system for apple surface defect detection. *Computers and Electronics in Agriculture*, 215-223. doi:https://doi.org/10.1016/S0168-1699(02)00093-5

Robert Gattshall. (2022). What is Backpressure and How Should We Calculate It? *Plastics Technologies*.

Yeong-Eun Yoo, Sang-Won Woo, Sun Kyoung Kim. (2012). Injection Molding Without Prior Drying Process by the Gas Counter Pressure. *Polymer Engineering and Science*, 2417-2423. doi:https://doi.org/10.1002/pen.23196

Table of Figures

List of Tables